 CMES, vol.28, no.1, pp.15-38, 2008

# Finite Rotation Geometrically Exact Four-Node Solid-Shell Element with Seven Displacement Degrees of Freedom

**G. M. Kulikov**[1] **and S. V. Plotnikova**[1]

**Abstract:** This paper presents a robust non-linear geometrically exact four-node solid-shell element based on the first-order seven-parameter equivalent single-layer theory, which permits us to utilize the 3D constitutive equations. The term "geometrically exact" reflects the fact that geometry of the reference surface is described by analytically given functions and displacement vectors are resolved in the reference surface frame. As fundamental shell unknowns six displacements of the outer surfaces and a transverse displacement of the midsurface are chosen. Such choice of displacements gives the possibility to derive strain-displacement relationships, which are invariant under arbitrarily large rigid-body shell motions in a convected curvilinear coordinate system. To avoid shear and membrane locking and have no spurious zero energy modes, the assumed strain and stress resultant fields are invoked. To improve a geometrically non-linear shell response, the modified ANS method is applied. Additionally, analytical integration throughout the element is employed to evaluate the tangent stiffness matrix. As a result, the present finite rotation solid-shell element formulation allows using coarse meshes and very large load increments.

**Keyword:** geometrically exact solid-shell element, finite rotations, seven-parameter shell formulation

## 1 Introduction

In recent years, a large number of works has been carried out on the 3D continuum-based non-linear finite elements that can handle the analysis of thin shells satisfactorily. These elements are typically defined by two layers of nodes at the bottom and top surfaces of the shell with three displacement degrees of freedom per node and known as isoparametric solid-shell elements [Kim and Lee (1988), Simo, Rifai and Fox (1990), Braun, Bischoff and Ramm (1994), Betsch and Stein (1995), Park, Cho and Lee (1995), Lee, Cho and Lee (2002), Sze, Chan and Pian (2002), Basar and Kintzel (2003)]. Unfortunately, a six-parameter solid-shell element formulation on the basis of the complete 3D constitutive equations is deficient because thickness locking occurs. This is due to the fact that the linear displacement field in the thickness direction results in a constant transverse normal strain, which in turn causes artificial stiffening of the element in the case of non-vanishing Poisson's ratios. To prevent thickness locking at the finite element level, the efficient enhanced assumed strain method [Braun, Bischoff and Ramm (1994), Betsch and Stein (1995)] can be applied. In order to circumvent a locking phenomenon at both mechanical and computational levels, the 3D constitutive equations have to be modified [Kim and Lee (1988), Park, Cho and Lee (1995), Sze, Chan and Pian (2002)]. However, the use of complete 3D constitutive laws within the shell analysis is of great importance for engineering applications. Thus, a seven-parameter solid-shell element formulation [Parisch (1995), Sansour (1995), Basar, Itskov and Eckstein (2000), El-Abbasi and Meguid (2000), Brank (2005)] is best suited for this purpose because such a formulation is optimal with respect to a number of degrees of freedom employed. We refer to review papers [Sze (2002), Bischoff, Wall, Bletzinger and Ramm (2004)], where the reader may find additional references on this subject.

In the isoparametric solid-shell element formulation, initial and deformed geometry are equally

[1] Tambov State Technical University, Sovetskaya Street 106, Tambov 392000, Russia

interpolated allowing one to describe rigid-body shell motions precisely. The development of non-linear isoparametric solid-shell elements was not straightforward. In order to overcome element deficiencies such as shear, membrane and curvature thickness locking, advanced finite element techniques including assumed natural strain, enhanced assumed strain and assumed stress or/and strain methods were applied. Still, the isoparametric solid-shell element formulation is computationally inefficient because stresses and strains are analyzed in the global and local orthogonal Cartesian coordinate systems, although the normalized element coordinates represent already convected curvilinear coordinates.

An alternative way is to develop non-linear *geometrically exact* solid-shell elements based on presentation of displacement vectors in the reference surface frame that finds its point of departure in papers of Kulikov (2004) and Kulikov and Plotnikova (2003, 2006, 2007), devoted to the six-parameter shell formulation. The term "geometrically exact" reflects the fact that coefficients of the first and second fundamental forms, and Christoffel symbols are taken exactly at every integration point. Therefore, no approximation of the reference surface is needed. The feature of the above geometrically exact solid-shell element formulation is that it is based on the strain-displacement relationships, which precisely represent arbitrarily large rigid-body motions in a convected curvilinear coordinate system.

Herein, a more general study on the basis of the finite rotation first-order seven-parameter shell theory is considered. As fundamental unknowns six displacements of the outer surfaces of the shell and an additional transverse displacement of the middle surface are chosen. Such choice of displacements gives the possibility to represent the proposed geometrically exact solid-shell element formulation in a compact form and to derive strain-displacement relationships, which are invariant again under large rigid-body motions. It should be mentioned that in some works developing the isoparametric solid-shell element formulation [see e.g. Parisch (1995)], displacement vectors of outer and middle surfaces are also utilized, but these vectors are resolved in the fixed orthogonal unit basis. An idea of this approach can be traced back to the contribution of Schoop (1986). However, in the developed seven-parameter shell theory selecting as unknowns the displacements of outer and middle surfaces has a principally another mechanical sense and allows us additionally to obtain strain-displacement relationships with aforementioned attractive properties.

The finite element formulation is based on the simple and efficient approximation of shells via four-node *curved* shell elements. To avoid shear and membrane locking and have no spurious zero energy modes, the assumed strain and stress resultant fields are invoked. This approach was developed for the linear and non-linear geometrically exact six-parameter solid-shell elements by Kulikov and Plotnikova (2002, 2003). Here, this assumed stress-strain formulation is extended to the geometrically exact multilayered four-node solid-shell element based on the seven-parameter equivalent single-layer shell theory, which allows us to utilize the 3D constitutive equations.

Taking into account that displacement vectors of outer and middle surfaces of the shell are resolved in the reference surface frame, the proposed geometrically exact solid-shell element formulation has computational advantages compared to the conventional isoparametric solid-shell element formulations, since it reduces the computational cost of numerical integration in the evaluation of the stiffness matrix. This is due to the fact that the element matrix developed requires only direct substitutions, i.e., no numerical matrix inversion is needed. This is unusual for the isoparametric hybrid/mixed shell element formulations. Additionally, we use the efficient 3D analytical integration [Kulikov and Plotnikova (2005), (2006) and (2007)] that gives the possibility to employ coarse meshes.

## 2 Kinematic description of undeformed shell

Let us consider a shell of thickness $h$. The shell can be defined as a 3D body of volume $V$ bounded by two outer surfaces $\Omega^-$ and $\Omega^+$, located at the distances $d^-$ and $d^+$ measured with respect to the reference surface $\Omega$ such that $h = d^- + d^+$, and the edge boundary surface $\boldsymbol{\varepsilon}$. The reference surface is assumed to be sufficiently smooth and without any singularities. As has been shown recently by Kulikov and Plotnikova (2007), this assumption cannot introduce any serious limitation in the shell theory because in the case of the robust choice of the reference surface we are able to model general surface geometry such as shell intersections and shell edges efficiently. Let the reference surface be referred to the convected curvilinear coordinates $\theta^1$ and $\theta^2$, whereas the coordinate $\theta^3$ is oriented along the unit vector $\mathbf{a}_3 = \mathbf{a}^3$ normal to the reference surface.

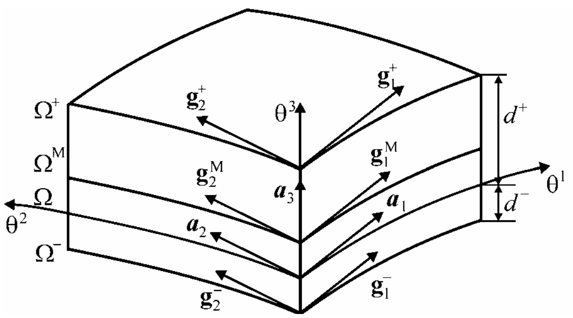


Figure 1: Geometry of the shell

Introduce in accordance with Figures 1 and 2 the following notations: $\mathbf{r} = \mathbf{r}\left(\theta^1, \theta^2\right)$ is the position vector of any point of the reference surface; $\mathbf{a}_\alpha = \mathbf{r}_{,\alpha}$ are the covariant base vectors of the reference surface; $\mathbf{a}^\beta$ are the contravariant base vectors of the reference surface defined by the standard relation $\mathbf{a}_\alpha \cdot \mathbf{a}^\beta = \delta_\alpha^\beta$; $a_{\alpha\beta} = \mathbf{a}_\alpha \cdot \mathbf{a}_\beta$ and $a^{\alpha\beta} = \mathbf{a}^\alpha \cdot \mathbf{a}^\beta$ are the covariant and contravariant components of the metric tensor of the reference surface; $a = \det\left[a_{\alpha\beta}\right]$ is the determinant of the metric tensor of the reference surface; $b_\alpha^\beta$ are the mixed components of the curvature tensor defined as

$$b_\alpha^\beta = -\mathbf{a}^\beta \cdot \mathbf{a}_{3,\alpha} \tag{1}$$

$\mathbf{R}$ is the position vector of any point in the shell body given by

$$\mathbf{R} = \mathbf{r} + \theta^3 \mathbf{a}_3 \tag{2}$$

in particular, position vectors of outer and middle surfaces are

$$\mathbf{R}^I = \mathbf{r} + z^I \mathbf{a}_3 \tag{3}$$

where $z^I$ are the transverse coordinates of outer and middle surfaces defined as

$$z^- = -d^-, \quad z^+ = d^+, \quad z^M = \frac{1}{2}\left(z^- + z^+\right) \tag{4}$$

$\mu_\alpha^\beta$ are the mixed components of the 3D shifter tensor expressed as

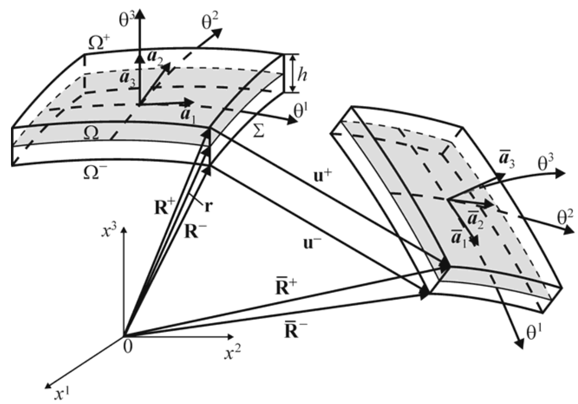


Figure 2: Initial and current configurations of the shell

$$\mu_\alpha^\beta = \delta_\alpha^\beta - \theta^3 b_\alpha^\beta \tag{5}$$

in particular, components of the shifter tensor at outer and middle surfaces are

$$\mu_\alpha^{I\beta} = \delta_\alpha^\beta - z^I b_\alpha^\beta \tag{6}$$

$\mathbf{g}_i$ are the covariant base vectors in the shell body defined as

$$\mathbf{g}_\alpha = \mathbf{R}_{,\alpha} = \mu_\alpha^\beta \mathbf{a}_\beta, \quad \mathbf{g}_3 = \mathbf{R}_{,3} = \mathbf{a}_3 \tag{7}$$

in particular, base vectors of outer and middle surfaces are

$$\mathbf{g}_\alpha^I = \mathbf{R}_{,\alpha}^I = \mu_\alpha^{I\beta} \mathbf{a}_\beta, \quad \mathbf{g}_3^I = \mathbf{a}_3 \tag{8}$$

$g_{ij}$ are the covariant components of the 3D metric tensor given by

$$g_{\alpha\beta} = \mathbf{g}_\alpha \cdot \mathbf{g}_\beta = \mu_\alpha^\gamma \mu_\beta^\delta a_{\gamma\delta}, \quad g_{i3} = \mathbf{g}_i \cdot \mathbf{g}_3 = \delta_{i3} \tag{9}$$

in particular, components of the metric tensors of outer and middle surfaces are

$$\begin{aligned} g_{\alpha\beta}^I &= \mathbf{g}_\alpha^I \cdot \mathbf{g}_\beta^I = \mu_\alpha^{I\gamma} \mu_\beta^{I\delta} a_{\gamma\delta}, \\ g_{i3}^I &= \mathbf{g}_i^I \cdot \mathbf{g}_3^I = \delta_{i3} \end{aligned} \tag{10}$$

$g = \det[g_{ij}]$ is the determinant of the 3D metric tensor; $g^I = \det\left[g^I_{ij}\right]$ are the determinants of the metric tensors of outer and middle surfaces; $\mu = \sqrt{g/a}$ is the determinant of the shifter tensor; $\mu^I = \sqrt{g^I/a}$ are the determinants of the shifter tensor at outer and middle surfaces; $(\ldots)_{,i}$ are the partial derivatives in $V$ with respect to coordinates $\theta^i$; $(\ldots)|_\alpha$ are the covariant derivatives in $\Omega$ with respect to coordinates $\theta^\alpha$. Here and in the following developments, Greek tensorial indices $\alpha$, $\beta$, $\gamma$, $\delta$ range from 1 to 2; Latin tensorial indices $i$, $j$, $m$, $n$ range from 1 to 3; Greek indices A, B identify the belonging of any quantity to the bottom and top surfaces and take values – and +; Latin indices $I, J$ identify the belonging of any quantity to the outer and middle surfaces and take values $-$, $+$ and M.

## 3 Kinematic description of deformed shell

Now, we introduce the first assumption for the proposed shell theory.

**Assumption 1.** The displacement field is approximated in the thickness direction according to the quadratic law

$$\mathbf{u} = \sum_I L^I \mathbf{u}^I \tag{11}$$

where $\mathbf{u}^I\left(\theta^1, \theta^2\right)$ are the displacement vectors of outer and middle surfaces; $L^I\left(\theta^3\right)$ are the Lagrange polynomials of the second order expressed as

$$\begin{aligned} L^- &= \frac{2}{h^2}\left(z^{\mathrm{M}} - \theta^3\right)\left(z^+ - \theta^3\right) \\ L^{\mathrm{M}} &= \frac{4}{h^2}\left(\theta^3 - z^-\right)\left(z^+ - \theta^3\right) \\ L^+ &= \frac{2}{h^2}\left(\theta^3 - z^-\right)\left(\theta^3 - z^{\mathrm{M}}\right) \end{aligned} \tag{12}$$

such that $L^I\left(z^J\right) = 1$ for $J = I$ and $L^I\left(z^J\right) = 0$ for $J \neq I$. Thus, we deal with the higher-order nine-parameter shell model because nine displacements of outer and middle surfaces are introduced by Eq. 11.

It is convenient to rewrite Eqs. 2 and 7 in more general forms

$$\mathbf{R} = \sum_I L^I \mathbf{R}^I, \quad \mathbf{R}^{\mathrm{M}} = \frac{1}{2}\left(\mathbf{R}^- + \mathbf{R}^+\right) \tag{13}$$

and

$$\mathbf{g}_\alpha = \sum_I L^I \mathbf{g}^I_\alpha, \quad \mathbf{g}^{\mathrm{M}}_\alpha = \frac{1}{2}\left(\mathbf{g}^-_\alpha + \mathbf{g}^+_\alpha\right) \tag{14a}$$

$$\mathbf{g}_3 = \sum_{\mathrm{A}} N^A \mathbf{g}^{\mathrm{A}}_3, \quad \mathbf{g}^{\mathrm{A}}_3 = \mathbf{a}_3 \tag{14b}$$

where $N^{\mathrm{A}}\left(\theta^3\right)$ are the polynomials of the first order defined as

$$N^- = \frac{1}{h}\left(z^+ - \theta^3\right), \quad N^+ = \frac{1}{h}\left(\theta^3 - z^-\right) \tag{15}$$

such that $N^{\mathrm{A}}\left(z^B\right) = 1$ for $\mathrm{B} = \mathrm{A}$ and $N^A\left(z^B\right) = 0$ for $\mathrm{B} \neq \mathrm{A}$.

Using Eqs. 11 and 13, we arrive at the formula for the position vector of the deformed shell

$$\overline{\mathbf{R}} = \mathbf{R} + \mathbf{u} = \sum_I L^I \overline{\mathbf{R}}^I \tag{16}$$

where $\overline{\mathbf{R}}^I\left(\theta^1, \theta^2\right)$ are the position vectors of outer and middle surfaces given by

$$\overline{\mathbf{R}}^I = \mathbf{R}^I + \mathbf{u}^I \tag{17}$$

The covariant base vectors in the current shell configuration are

$$\overline{\mathbf{g}}_\alpha = \overline{\mathbf{R}}_{,\alpha} = \sum_I L^I \overline{\mathbf{g}}^I_\alpha \tag{18a}$$

$$\overline{\mathbf{g}}_3 = \overline{\mathbf{R}}_{,3} = \sum_A N^{\mathrm{A}} \overline{\mathbf{g}}^{\mathrm{A}}_3 \tag{18b}$$

Here, $\overline{\mathbf{g}}^I_\alpha$ and $\overline{\mathbf{g}}^{\mathrm{A}}_3$ are the base vectors of outer and middle surfaces of the deformed shell expressed as

$$\overline{\mathbf{g}}^I_\alpha = \overline{\mathbf{R}}^I_{,\alpha} = \mathbf{g}^I_\alpha + \mathbf{u}^I_{,\alpha}, \quad \overline{\mathbf{g}}^{\mathrm{A}}_3 = \mathbf{a}_3 + \boldsymbol{\beta}^{\mathrm{A}} \tag{19}$$

where

$$\boldsymbol{\beta}^{\mathrm{A}} = \mathbf{u}_{,3}\left(z^A\right) \tag{20a}$$

that can be represented by using Eqs. 11 and 12 as follows:

$$\begin{aligned} \boldsymbol{\beta}^- &= \frac{1}{h}\left(-3\mathbf{u}^- + 4\mathbf{u}^{\mathrm{M}} - \mathbf{u}^+\right) \\ \boldsymbol{\beta}^+ &= \frac{1}{h}\left(\mathbf{u}^- - 4\mathbf{u}^{\mathrm{M}} + 3\mathbf{u}^+\right) \end{aligned} \tag{20b}$$

## 4 Strain-displacement relationships

The Green-Lagrange strain tensor can be written as

$$2\varepsilon_{ij} = \overline{\mathbf{g}}_i \cdot \overline{\mathbf{g}}_j - \mathbf{g}_i \cdot \mathbf{g}_j \tag{21}$$

Substituting base vectors (14) and (18) into relationships (21), one finds

$$2\varepsilon_{\alpha\beta} = \sum_{I,J} L^I L^J \left( \mathbf{u}^I_{,\alpha} \cdot \mathbf{g}^J_\beta + \mathbf{u}^J_{,\beta} \cdot \mathbf{g}^I_\alpha + \mathbf{u}^I_{,\alpha} \cdot \mathbf{u}^J_{,\beta} \right)$$

$$2\varepsilon_{\alpha 3} = \sum_{\mathrm{A},I} N^{\mathrm{A}} L^I \left( \mathbf{u}^I_{,\alpha} \cdot \mathbf{a}_3 + \boldsymbol{\beta}^{\mathrm{A}} \cdot \mathbf{g}^I_\alpha + \boldsymbol{\beta}^{\mathrm{A}} \cdot \mathbf{u}^I_{,\alpha} \right)$$

$$2\varepsilon_{33} = \sum_{\mathrm{A},\mathrm{B}} N^{\mathrm{A}} N^{\mathrm{B}} \left( \beta^{\mathrm{A}} \cdot \mathbf{a}_3 + \boldsymbol{\beta}^{\mathrm{B}} \cdot \mathbf{a}_3 + \boldsymbol{\beta}^{\mathrm{A}} \cdot \boldsymbol{\beta}^{\mathrm{B}} \right) \tag{22}$$

It is seen from Eqs. 12, 15 and 22 that in-plane strains $\varepsilon_{\alpha\beta}$ are the polynomials of the fourth order, transverse shear strains $\varepsilon_{\alpha 3}$ are the polynomials of the third order and a transverse normal strain $\varepsilon_{33}$ is the polynomial of the second order. To simplify the higher-order nine-parameter shell formulation, we introduce the next assumption.

**Assumption 2.** From the mechanical point of view it is convenient to assume that all components of the Green-Lagrange strain tensor are distributed through the thickness of the shell according to the displacement distribution (11), i.e.,

$$\check{\varepsilon}_{ij} = \sum_I L^I \varepsilon^I_{ij} \tag{23}$$

where $\varepsilon^I_{ij} = \varepsilon_{ij}\left(z^I\right)$ are the *exact values* of Green-Lagrange strains at the outer and middle surfaces defined as

$$2\varepsilon^I_{\alpha\beta} = \mathbf{u}^I_{,\alpha} \cdot \mathbf{g}^I_\beta + \mathbf{u}^I_{,\beta} \cdot \mathbf{g}^I_\alpha + \mathbf{u}^I_{,\alpha} \cdot \mathbf{u}^I_{,\beta}$$

$$2\varepsilon^I_{\alpha 3} = \mathbf{u}^I_{,\alpha} \cdot \mathbf{a}_3 + \boldsymbol{\beta}^I \cdot \mathbf{g}^I_\alpha + \boldsymbol{\beta}^I \cdot \mathbf{u}^I_{,\alpha}$$

$$2\varepsilon^I_{33} = 2\beta^I \cdot \mathbf{a}_3 + \boldsymbol{\beta}^I \cdot \boldsymbol{\beta}^I \tag{24}$$

Here, an additional notation (see Eq. 20) has been introduced

$$\boldsymbol{\beta}^{\mathrm{M}} = \mathbf{u}_{,3}\left(z^{\mathrm{M}}\right) = \frac{1}{h}\left(\mathbf{u}^+ - \mathbf{u}^-\right) \tag{25}$$

Actually, this assumption implies that now all strain components $\check{\varepsilon}_{ij}$ are the polynomials of the second order that simplifies sufficiently the non-linear higher-order nine-parameter shell formulation.

**Remark 1.** It can be verified by using Eqs. 12 and 15 that components of the simplified and exact Green-Lagrange strain tensors satisfy linking conditions

$$\check{\varepsilon}_{ij}\left(z^I\right) = \varepsilon_{ij}\left(z^I\right) = \varepsilon^I_{ij} \tag{26}$$

These links are illustrated by means of Figure 3. It should be also noticed that the non-uniform distribution of the transverse normal strain in the thickness direction permits us to utilize 3D constitutive laws. In principle, the linear strain distribution is sufficient for this purpose [Parisch (1995), Sansour (1995)].

We next represent displacement vectors of outer and middle surfaces as follows:

$$\mathbf{u}^I = u^I_i \mathbf{a}^i \tag{27}$$

It is seen that displacement vectors are resolved in the contravariant reference surface basis $\mathbf{a}^i$ that allows us to reduce the costly numerical integration by evaluating the stiffness matrix [Kulikov and Plotnikova (2006) and (2007)]. The derivatives of displacement vectors $\boldsymbol{\beta}^I$ from Eqs. 20 and 25 can be represented in a similar way

$$\boldsymbol{\beta}^I = \beta^I_i \mathbf{a}^i \tag{28a}$$

where

$$\beta^-_i = \frac{1}{h}\left(-3u^-_i + 4u^{\mathrm{M}}_i - u^+_i\right)$$

$$\beta^+_i = \frac{1}{h}\left(u^-_i - 4u^{\mathrm{M}}_i + 3u^+_i\right)$$

$$\beta^{\mathrm{M}}_i = \frac{1}{h}\left(u^+_i - u^-_i\right) \tag{28b}$$

The derivatives of displacement vectors of outer and middle surfaces are written as

$$\mathbf{u}^I_{,\alpha} = u^I_i|_\alpha \mathbf{a}^i \tag{29}$$

$$u^I_i|_\alpha = u^I_{i,\alpha} - \Gamma^j_{i\alpha} u^I_j \tag{30}$$

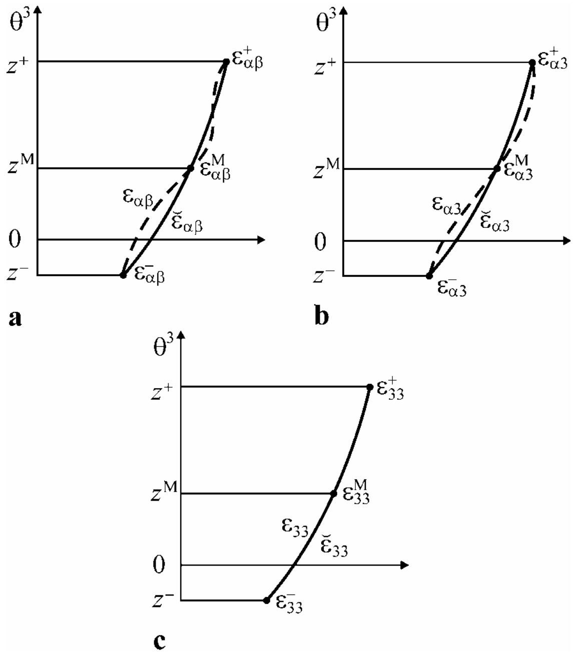


Figure 3: Approximate (—) and exact (– –) distributions of (a) in-plane, (b) transverse shear and (c) transverse normal strains through the thickness of the shell for the higher-order nine-parameter shell theory

where $\Gamma^j_{i\alpha}$ are the Christoffel symbols defined as

$$\Gamma^i_{\alpha\beta} = \mathbf{a}^i \cdot \mathbf{a}_{\alpha,\beta}, \quad \Gamma^\beta_{3\alpha} = -b^\beta_\alpha, \quad \Gamma^3_{3\alpha} = 0 \tag{31}$$

Substituting Eqs. 8, 28 and 29 into strain-displacement relationships (24), we arrive at a scalar form of these relationships

$$2\varepsilon^I_{\alpha\beta} = \mu^{I\gamma}_\beta u^I_\gamma|_\alpha + \mu^{I\gamma}_\alpha u^I_\gamma|_\beta + a^{ij} u^I_i|_\alpha u^I_j|_\beta$$

$$2\varepsilon^I_{\alpha 3} = u^I_3|_\alpha + \mu^{I\gamma}_\alpha \beta^I_\gamma + a^{ij} \beta^I_i u^I_j|_\alpha$$

$$2\varepsilon^I_{33} = 2\beta^I_3 + a^{ij} \beta^I_i \beta^I_j \tag{32}$$

where for convenience it has been introduced an additional notation $a^{i3} = \delta^{i3}$. In orthogonal curvilinear surface coordinates, the strain-displacement relationships (32) can be represented in a simpler form (see Appendix A).

We now formulate the fundamental statement concerning the Green-Lagrange strain tensor developed.

**Proposition 1.**[1] The Green-Lagrange strain components (23) are objective, i.e., they represent precisely large rigid-body shell motions in any convected curvilinear coordinate system.

**Proof.** The large rigid-body shell displacements can be defined as

$$(\mathbf{u})^{\text{Rigid}} = \Delta + \Phi\mathbf{R} - \mathbf{R} \tag{33}$$

where $\Delta = \Delta_i a^i$ is the constant displacement (translation) vector; $\Phi$ is the orthogonal rotation matrix (see e.g. Kulikov, 2004). In particular, rigid-body shell displacements of outer and middle surfaces are written as

$$\left(\mathbf{u}^I\right)^{\text{Rigid}} = \Delta + \Phi\mathbf{R}^I - \mathbf{R}^I \tag{34}$$

The derivatives of the translation vector and the rotation matrix with respect to convected coordinates are zero, that is,

$$\Delta_{,\alpha} = \mathbf{0} \text{ and } \Phi_{,\alpha} = \mathbf{0} \tag{35}$$

Allowing for Eqs. 8 and 35, the derivatives of displacement vectors (34) are expressed as

$$\left(\mathbf{u}^I_{,\alpha}\right)^{\text{Rigid}} = \Phi\mathbf{g}^I_\alpha - \mathbf{g}^I_\alpha \tag{36}$$

Using Eqs. 20, 25 and 34, and taking into account formulas for the position vectors of outer and middle surfaces (3) and (13) as well, one obtains

$$\left(\boldsymbol{\beta}^I\right)^{\text{Rigid}} = \Phi\mathbf{a}_3 - \mathbf{a}_3 \tag{37}$$

It may be verified by employing Eqs. 36 and 37 that strains of outer and middle surfaces (24) are all zero in a general large rigid-body shell motion:

$$2\left(\varepsilon^I_{ij}\right)^{\text{Rigid}} = \left(\Phi\mathbf{g}^I_i\right) \cdot \left(\Phi\mathbf{g}^I_j\right) - \mathbf{g}^I_i \cdot \mathbf{g}^I_j = 0 \tag{38}$$

This conclusion is true because the orthogonal transformation retains the scalar product of vectors. Therefore, due to Eq. 38 the simplified Green-Lagrange strains (23) exactly represent arbitrarily large rigid-body motions, i.e.,

$$(\breve{\varepsilon}_{ij})^{\text{Rigid}} = 0 \tag{39}$$

[1] This proposition has been proved recently for the nonlinear higher-order nine-parameter plate theory by Kulikov (2007)

that completes the proof.

Thus, we have derived strain-displacement relationships (23) and (32) of the higher-order nine-parameter shell model, which exactly represent arbitrarily large rigid-body motions in a convected curvilinear coordinate system. However, for the better computational efficiency we have to reduce a number of degrees of freedom. It is apparent that a first-order[2] seven-parameter shell model is best suited for this purpose because such a model allows one to utilize the 3D constitutive equations and is optimal with respect to a number of degrees of freedom employed [Parisch (1995), Sansour (1995)].

To diminish a number of unknown displacements, we should accept an additional assumption.

**Assumption 3.** It is assumed, first, that in-plane and transverse normal components of the Green-Lagrange strain tensor are linear, whereas transverse shear components are constant through the thickness of the shell:

$$\hat{\varepsilon}_{\alpha\beta} = \sum_{\mathrm{A}} N^{\mathrm{A}} \varepsilon^{\mathrm{A}}_{\alpha\beta} \tag{40a}$$

$$\hat{\varepsilon}_{\alpha 3} = \varepsilon^{\mathrm{a}}_{\alpha 3} = \frac{1}{2}\left(\varepsilon^{-}_{\alpha 3} + \varepsilon^{+}_{\alpha 3}\right) \tag{40b}$$

$$\hat{\varepsilon}_{33} = \sum_{\mathrm{A}} N^{\mathrm{A}} \varepsilon^{\mathrm{A}}_{33} \tag{40c}$$

where $\varepsilon^{\mathrm{a}}_{\alpha 3}$ are the average values of transverse shear strains at the bottom and top surfaces. Second, the in-plane displacements are considered to be linear, while the transverse displacement remains quadratic in the thickness direction, that is,

$$u_\alpha = \sum_{\mathrm{A}} N^{\mathrm{A}} u^{\mathrm{A}}_\alpha \tag{41a}$$

$$u_3 = \sum_{I} L^I u^I_3 \tag{41b}$$

**Remark 2.** It may be shown by using Eqs. 22 and 40, and taking Eqs. 12, 15 and 24 into account that in-plane and transverse normal components of the simplified and exact Green-Lagrange strain tensors satisfy linking conditions at the bottom and top surfaces

$$\hat{\varepsilon}_{\alpha\beta}\left(z^A\right) = \varepsilon_{\alpha\beta}\left(z^A\right) = \varepsilon^{\mathrm{A}}_{\alpha\beta} \tag{42a}$$

$$\hat{\varepsilon}_{33}\left(z^A\right) = \varepsilon_{33}\left(z^A\right) = \varepsilon^{\mathrm{A}}_{33} \tag{42b}$$

This fact is illustrated in Figure 4.

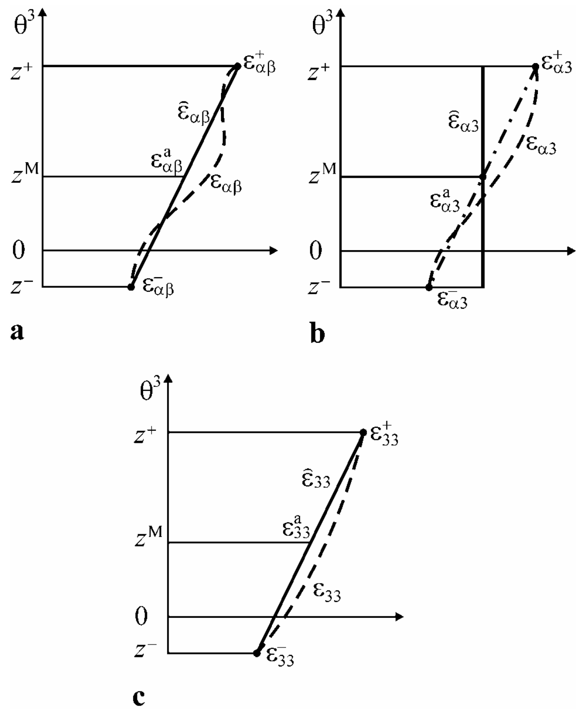


Figure 4: Approximate (—) and exact (– –) distributions of (a) in-plane, (b) transverse shear and (c) transverse normal strains through the thickness of the shell for the first-order seven-parameter shell theory

As we shall see later, strains (40) in conjunction with relationships (32) provide a very simple and convenient way to overcome thickness locking in the case of utilizing the complete 3D constitutive equations because only seven displacements $u^-_i$, $u^+_i$ and $u^M_3$ are introduced into the shell formulation.

## 5 Hu-Washizu variational equation for multilayered shell

The first-order seven-parameter shell theory developed is based on the assumed approximations of displacements (41) and displacement-

[2] This is due to the linear strain distribution through the thickness of the shell

dependent strains $\hat{\varepsilon}_{ij}$ (Eq. 40) in the thickness direction. Additionally, to circumvent shear and membrane locking, we introduce the similar approximation for the assumed displacement-independent strains

$$\varepsilon_{\alpha\beta}^{\mathrm{AS}} = \sum_{\mathrm{A}} N^{\mathrm{A}} E_{\alpha\beta}^{\mathrm{A}} \tag{43a}$$

$$\varepsilon_{\alpha 3}^{\mathrm{AS}} = E_{\alpha 3} \tag{43b}$$

$$\varepsilon_{33}^{\mathrm{AS}} = \sum_{\mathrm{A}} N^{\mathrm{A}} E_{33}^{\mathrm{A}} \tag{43c}$$

Now, we consider a more general shell configuration built up by the arbitrary superposition across the wall thickness of $NL$ layers of thickness $h_k$ (Figure 5). The $k$th layer may be defined as a 3D body of volume $V_k$ bounded by two surfaces $\Omega_{k-1}$ and $\Omega_k$, located at the distances $z_{k-1}$ and $z_k$ measured with respect to the reference surface $\boldsymbol{\Omega}$, and the edge boundary surface $\boldsymbol{\varepsilon}_k$. The constituent layers of the shell are supposed to be rigidly joined, so that no slip on contact surfaces and no separation of layers can occur. The material of each layer is assumed to be linearly elastic, anisotropic, homogeneous or fiber-reinforced, such that in each point there is a single surface of elastic symmetry parallel to the reference surface. Here and in the following developments, the index $k$ identifies the belonging of any quantity to the $k$th layer and runs from 1 to $NL$.

For the sake of simplicity, our discussion is limited to the case of zero body forces and conservative surface loading. To arrive at the assumed stress-strain element formulation, we consider the Hu-Washizu functional

$$J_{\mathrm{HW}} = \iint_{\Omega} \sum_k \int_{z_{k-1}}^{z_k} \left[ \frac{1}{2} \varepsilon_{ij}^{\mathrm{AS}} C_k^{ijmn} \varepsilon_{mn}^{\mathrm{AS}} \right. \\ \left. - S_k^{ij} \left( \varepsilon_{ij}^{\mathrm{AS}} - \hat{\varepsilon}_{ij} \right) \right] \mu \sqrt{a} d\theta^1 d\theta^2 d\theta^3 \\ - \iint_{\Omega} \left( \mu^+ p_+^i u_i^+ - \mu^- p_-^i u_i^- \right) \sqrt{a} d\theta^1 d\theta^2 - W^{\mathrm{ext}} \tag{44}$$

where $S_k^{ij}$ are the contravariant components of the second Piola-Kirchhoff stress tensor of the $k$th layer; $C_k^{ijmn}$ are the contravariant components of the material tensor of the $k$th layer; $W^{\mathrm{ext}}$ is the work done by external loads acting on the edge boundary surface $\boldsymbol{\varepsilon}$; $p_-^i$ and $p_+^i$ are the contravariant components of the traction vectors $\mathbf{p}^-$ and $\mathbf{p}^+$ applied to the bottom and top surfaces.

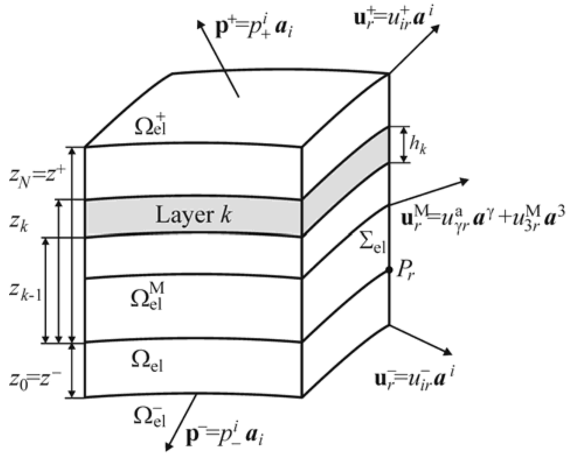


Figure 5: Geometrically exact multilayered seven-parameter shell element, where $P_r$ denotes the element node

Substituting assumed approximations of displacements and strains (40), (41) and (43) in the thickness direction into functional (44) and introducing stress-resultants

$$H_{\mathrm{A}}^{\alpha\beta} = \sum_k \int_{z_{k-1}}^{z_k} \mu S_k^{\alpha\beta} N^{\mathrm{A}} d\theta^3 \\ H_{\mathrm{A}}^{33} = \sum_k \int_{z_{k-1}}^{z_k} \mu S_k^{33} N^{\mathrm{A}} d\theta^3 \\ H^{\alpha 3} = \sum_k \int_{z_{k-1}}^{z_k} \mu S_k^{\alpha 3} d\theta^3 \tag{45}$$

and invoking the stationarity of this functional with respect to independent variables, one derives the following mixed variational equation for the geometrically exact solid-shell element formulation:

$$\iint\limits_{\tilde{\Omega}_{\mathrm{el}}} \Big[\delta\mathbf{E}^{\mathrm{T}}(\mathbf{H}-\mathbf{D}\mathbf{E})+\delta\mathbf{H}^{\mathrm{T}}(\mathbf{E}-\boldsymbol{\varepsilon}) - \delta\boldsymbol{\varepsilon}^{\mathrm{T}}\mathbf{H}+\delta\mathbf{V}^{\mathrm{T}}\mathbf{P}\Big]\sqrt{a}\Lambda d\xi^1 d\xi^2+\delta W_{\mathrm{el}}^{\mathrm{ext}} = 0 \quad (46)$$

where $\tilde{\Omega}_{\mathrm{el}} = [-1, 1]\times[-1, 1]$ is the biunit square in $(\xi^1, \xi^2)$ -space (see Figure 6); $\Lambda$ is the determinant of the transformation matrix; $\mathbf{V}$ is the displacement vector[3]; $\mathbf{P}$ is the surface traction vector; $\boldsymbol{\varepsilon}$ and $\mathbf{E}$ are the displacement-dependent and displacement-independent strain vectors; $\mathbf{H}$ is the stress resultant vector; $\mathbf{D}$ is the laminate constitutive stiffness matrix given by

$$\Lambda = \det\left[\frac{\partial\theta^\beta}{\partial\xi^\alpha}\right] \quad (47)$$

$$\mathbf{V} = \left[u_1^- \; u_2^- \; u_3^- \; u_1^+ \; u_2^+ \; u_3^+ \; u_3^{\mathrm{M}}\right]^{\mathrm{T}}$$

$$\mathbf{P} = \left[-\mu^- p_-^1 \;\; -\mu^- p_-^2 \;\; -\mu^- p_-^3 \;\; \mu^+ p_+^1 \;\; \mu^+ p_+^2 \;\; \mu^+ p_+^3 \;\; 0\right]^{\mathrm{T}}$$

$$\boldsymbol{\varepsilon} = \left[\varepsilon_{11}^- \; \varepsilon_{11}^+ \; \varepsilon_{22}^- \; \varepsilon_{22}^+ \; \varepsilon_{33}^- \; \varepsilon_{33}^+ \; 2\varepsilon_{12}^- \; 2\varepsilon_{12}^+ \; 2\varepsilon_{13}^{\mathrm{a}} \; 2\varepsilon_{23}^{\mathrm{a}}\right]^{\mathrm{T}}$$

$$\mathbf{E} = \left[E_{11}^- \; E_{11}^+ \; E_{22}^- \; E_{22}^+ \; E_{33}^- \; E_{33}^+ \; 2E_{12}^- \; 2E_{12}^+ \; 2E_{13} \; 2E_{23}\right]^{\mathrm{T}}$$

$$\mathbf{H} = \left[H_-^{11} \; H_+^{11} \; H_-^{22} \; H_+^{22} \; H_-^{33} \; H_+^{33} \; H_-^{12} \; H_+^{12} \; H^{13} \; H^{23}\right]^{\mathrm{T}}$$

$$\mathbf{D} = \begin{bmatrix}
D_{00}^{1111} & D_{01}^{1111} & D_{00}^{1122} & D_{01}^{1122} & D_{00}^{1133} & D_{01}^{1133} & D_{00}^{1112} & D_{01}^{1112} & 0 & 0 \\
 & D_{11}^{1111} & D_{01}^{1122} & D_{11}^{1122} & D_{01}^{1133} & D_{11}^{1133} & D_{01}^{1112} & D_{11}^{1112} & 0 & 0 \\
 & & D_{00}^{2222} & D_{01}^{2222} & D_{00}^{2233} & D_{01}^{2233} & D_{00}^{2212} & D_{01}^{2212} & 0 & 0 \\
 & & & D_{11}^{2222} & D_{01}^{2233} & D_{11}^{2233} & D_{01}^{2212} & D_{11}^{2212} & 0 & 0 \\
 & & & & D_{00}^{3333} & D_{01}^{3333} & D_{00}^{3312} & D_{01}^{3312} & 0 & 0 \\
 & & & & & D_{11}^{3333} & D_{01}^{3312} & D_{11}^{3312} & 0 & 0 \\
 & & & & & & D_{00}^{1212} & D_{01}^{1212} & 0 & 0 \\
 & & & & & & & D_{11}^{1212} & 0 & 0 \\
 & & & & & & & & D^{1313} & D^{1323} \\
\text{sym.} & & & & & & & & & D^{2323}
\end{bmatrix}$$

The elements of the constitutive stiffness matrix are

$$D_{r_1 r_2}^{ijmn} = \sum_k \int\limits_{z_{k-1}}^{z_k} \mu C_k^{ijmn} \left(N^-\right)^{2-r_1-r_2} \left(N^+\right)^{r_1+r_2} d\theta^3$$

$$D^{\alpha 3\beta 3} = D_{00}^{\alpha 3\beta 3} + 2D_{01}^{\alpha 3\beta 3} + D_{11}^{\alpha 3\beta 3} \quad (48)$$

Throughout this and next sections indices $r_1$ and $r_2$ take the values 0 and 1.

**Remark 3.** To carry out the *exact* analytical integration in Eq. 48, the determinant of the 3D shifter tensor can be approximated through the shell thickness by applying the linear law that has already been used in previous developments:

$$\mu = \sum_{\mathrm{A}} N^{\mathrm{A}} \mu^{\mathrm{A}} \quad (49)$$

In practice, for thin-walled structures the simplest approximation may be employed

$$\mu = \mu^{\mathrm{a}} = \frac{1}{2}\left(\mu^- + \mu^+\right) \quad (50)$$

For very thin shells one can assume that metrics of all surfaces parallel to the reference surface are identical and equal to the metric of the midsurface [see e.g. works of Kulikov and Plotnikova

[3] From this point, any vector of order $M$ means the standard column matrix of order $M\times 1$

(2002, 2003, 2007)]. This implies that in the case of choosing the midsurface as a reference surface the simplest approximation $\mu = 1$ may be utilized.

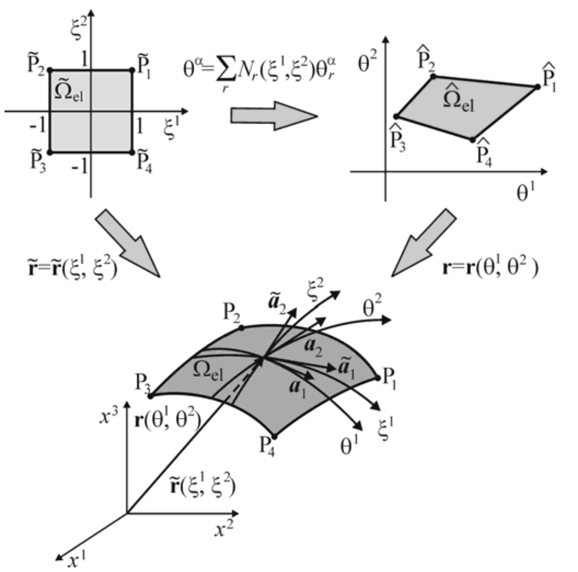


Figure 6: Biunit square in $(\xi^1, \xi^2)$ -space mapped into the geometrically exact four-node shell element in $(x^1, x^2, x^3)$-space

## 6 Assumed stress-strain finite element formulation

For the four-node *curved* solid-shell element the displacement field (see Appendix A) is approximated according to the standard $C^0$ interpolation

$$\mathbf{V} = \sum_r N_r \mathbf{V}_r \tag{51a}$$

$$\mathbf{V} = \left[\dot{u}_1^- \ \dot{u}_2^- \ \dot{u}_3^- \ \dot{u}_1^+ \ \dot{u}_2^+ \ \dot{u}_3^+ \ \dot{u}_3^{\mathrm{M}}\right]$$

$$\mathbf{V}_r = \left[\dot{u}_{1r}^- \ \dot{u}_{2r}^- \ \dot{u}_{3r}^- \ \dot{u}_{1r}^+ \ \dot{u}_{2r}^+ \ \dot{u}_{3r}^+ \ \dot{u}_{3r}^{\mathrm{M}}\right]^{\mathrm{T}} \tag{51b}$$

where $\mathbf{V}_r$ are the displacement vectors of the element nodes; $N_r(\xi^1, \xi^2)$ are the bilinear shape functions of the element and the index $r$ denotes a number of nodes and ranges from 1 to 4. The surface traction vector is also assumed to vary bilinearly inside the element.

The displacement approximation (51) can be rewritten as

$$\mathbf{V} = \sum_{r_1, r_2} \left(\xi^1\right)^{r_1} \left(\xi^2\right)^{r_2} \mathbf{V}^{r_1 r_2} \quad \text{for } r_1, \ r_2 = 0, 1$$
$$\mathbf{V}^{00} = \frac{1}{4}\left(\mathbf{V}_1 + \mathbf{V}_2 + \mathbf{V}_3 + \mathbf{V}_4\right)$$
$$\mathbf{V}^{10} = \frac{1}{4}\left(\mathbf{V}_1 - \mathbf{V}_2 - \mathbf{V}_3 + \mathbf{V}_4\right)$$
$$\mathbf{V}^{01} = \frac{1}{4}\left(\mathbf{V}_1 + \mathbf{V}_2 - \mathbf{V}_3 - \mathbf{V}_4\right)$$
$$\mathbf{V}^{11} = \frac{1}{4}\left(\mathbf{V}_1 - \mathbf{V}_2 + \mathbf{V}_3 - \mathbf{V}_4\right) \tag{52}$$

that is best suited for the implementation of the analytical integration throughout the element.

The use of Eq. 52 in Eqs. A8 and A9 leads to the biquadratic interpolation for displacement-dependent strains

$$\boldsymbol{\varepsilon} = \sum_{s_1, s_2} \left(\xi^1\right)^{s_1} \left(\xi^2\right)^{s_2} E^{s_1 s_2} \tag{53a}$$

$$\boldsymbol{\varepsilon} = \left[\dot{\varepsilon}_{11}^- \ \dot{\varepsilon}_{11}^+ \ \dot{\varepsilon}_{22}^- \ \dot{\varepsilon}_{22}^+ \ \dot{\varepsilon}_{33}^- \ \dot{\varepsilon}_{33}^+ \ 2\dot{\varepsilon}_{12}^- \ 2\dot{\varepsilon}_{12}^+ \ 2\dot{\varepsilon}_{13}^{\mathrm{a}} \ 2\dot{\varepsilon}_{23}^{\mathrm{a}}\right]^{\mathrm{T}}$$

$$\boldsymbol{\varepsilon}^{s_1 s_2} = \left[\dot{\varepsilon}_{11}^{-s_1 s_2} \ \dot{\varepsilon}_{11}^{+s_1 s_2} \ \dot{\varepsilon}_{22}^{-s_1 s_2} \ \dot{\varepsilon}_{22}^{+s_1 s_2} \ \dot{\varepsilon}_{33}^{-s_1 s_2} \ \dot{\varepsilon}_{33}^{+s_1 s_2} \ 2\dot{\varepsilon}_{12}^{-s_1 s_2} \ 2\dot{\varepsilon}_{12}^{+s_1 s_2} \ 2\dot{\varepsilon}_{13}^{\mathrm{a} s_1 s_2} \ 2\dot{\varepsilon}_{23}^{\mathrm{a} s_1 s_2}\right]^{\mathrm{T}} \tag{53b}$$

where $\boldsymbol{\varepsilon}^{s_1 s_2}$ are the mode strain vectors, which are constant throughout the element and evaluated in Appendix B by means of non-conventional schemes [Kulikov and Plotnikova (2006) and (2007)], and the superscripts $s_1$ and $s_2$ run from 0 to 2.

It is convenient to introduce a displacement vector of the shell element of order 28 as follows:

$$\mathbf{U} = \left[\mathbf{V}_1^{\mathrm{T}} \ \mathbf{V}_2^{\mathrm{T}} \ \mathbf{V}_3^{\mathrm{T}} \ \mathbf{V}_4^{\mathrm{T}}\right]^{\mathrm{T}} \tag{54}$$

Using this notation in Eqs. B1-B4, we get a more suitable form for the mode strain vectors (53b):

$$\boldsymbol{\varepsilon}^{s_1 s_2} = \mathbf{B}^{s_1 s_2}\mathbf{U} + \left(\mathbf{A}^{s_1 s_2}\mathbf{U}\right)\mathbf{U} = \left(\mathbf{B}^{s_1 s_2} + \mathbf{A}^{s_1 s_2}\mathbf{U}\right)\mathbf{U} \tag{55}$$

where $\mathbf{B}^{s_1 s_2}$ are the *constant* matrices of order $10 \times 28$ corresponding to the linear strain-displacement transformation (B2) such that

$\mathbf{B}^{s_1s_2} = \mathbf{0}$ for $s_1 = 2$ or $s_2 = 2$; $\mathbf{A}^{s_1s_2}$ are the *constant* 3D arrays of order $10\times 28\times 28$ corresponding to the non-linear strain-displacement transformation (B3); $\mathbf{A}^{s_1s_2}\mathbf{U}$ are the matrices of order $10\times 28$ whose elements are defined as

$$(\mathbf{A}^{s_1s_2}\mathbf{U})_{lp} = \sum_q A^{s_1s_2}_{lpq} U_q \tag{56a}$$

$$A^{s_1s_2}_{lpq} = A^{s_1s_2}_{lqp} \text{ for } l = \overline{1,10} \text{ and } p,q = \overline{1,28} \tag{56b}$$

To avoid shear and membrane locking and have no spurious zero energy modes, the assumed displacement-independent strain and stress resultant fields [Kulikov and Plotnikova (2003)] inside the element are introduced

$$\mathbf{E} = \sum_{r_1,r_2} (\xi^1)^{r_1} (\xi^2)^{r_2} \mathbf{Q}^{r_1r_2}\mathbf{E}^{r_1r_2} \tag{57a}$$

$$\mathbf{E}^{00} = \left[E^{-00}_{11}\ E^{+00}_{11}\ E^{-00}_{22}\ E^{+00}_{22}\ E^{-00}_{33}\ E^{+00}_{33}\ 2E^{-00}_{12}\ 2E^{+00}_{12}\ 2E^{00}_{13}\ 2E^{00}_{23}\right]^{\mathrm{T}}$$

$$\mathbf{E}^{01} = \left[E^{-01}_{11}\ E^{+01}_{11}\ E^{-01}_{33}\ E^{+01}_{33}\ 2E^{01}_{13}\right]^{\mathrm{T}}$$

$$\mathbf{E}^{10} = \left[E^{-10}_{22}\ E^{+10}_{22}\ E^{-10}_{33}\ E^{+10}_{33}\ 2E^{10}_{23}\right]^{\mathrm{T}}$$

$$\mathbf{E}^{11} = \left[E^{-11}_{33}\ E^{+11}_{33}\ \right]^{\mathrm{T}}$$

$$\mathbf{H} = \sum_{r_1,\,r_2} (\xi^1)^{r_1} (\xi^2)^{r_2} \mathbf{Q}^{r_1\,r_2}\mathbf{H}^{r_1\,r_2} \tag{57b}$$

$$\mathbf{H}^{00} = \left[H^{-00}_{11}\ H^{+00}_{11}\ H^{-00}_{22}\ H^{+00}_{22}\ H^{-00}_{33}\ H^{+00}_{33}\ H^{-00}_{12}\ H^{+00}_{12}\ H^{00}_{13}\ H^{00}_{23}\right]^{\mathrm{T}}$$

$$\mathbf{H}^{01} = \left[H^{-01}_{11}\ H^{+01}_{11}\ H^{-01}_{33}\ H^{+01}_{33}\ H^{01}_{13}\right]^{\mathrm{T}}$$

$$\mathbf{H}^{10} = \left[H^{-10}_{22}\ H^{+10}_{22}\ H^{-10}_{33}\ H^{+10}_{33}\ H^{10}_{23}\right]^{\mathrm{T}}$$

$$\mathbf{H}^{11} = \left[H^{-11}_{33}\ H^{+11}_{33}\ \right]^{\mathrm{T}}$$

$$\mathbf{Q}^{01} = \begin{bmatrix} 1&0&0&0&0\\ 0&1&0&0&0\\ 0&0&0&0&0\\ 0&0&0&0&0\\ 0&0&1&0&0\\ 0&0&0&1&0\\ 0&0&0&0&0\\ 0&0&0&0&0\\ 0&0&0&0&1\\ 0&0&0&0&0 \end{bmatrix}$$

$$\mathbf{Q}^{10} = \begin{bmatrix} 0&0&0&0&0\\ 0&0&0&0&0\\ 1&0&0&0&0\\ 0&1&0&0&0\\ 0&0&1&0&0\\ 0&0&0&1&0\\ 0&0&0&0&0\\ 0&0&0&0&0\\ 0&0&0&0&0\\ 0&0&0&0&1 \end{bmatrix}$$

$$\mathbf{Q}^{11} = \begin{bmatrix} 0&0&0&0&1&0&0&0&0&0\\ 0&0&0&0&0&1&0&0&0&0 \end{bmatrix}^{\mathrm{T}} \tag{57c}$$

where $\mathbf{Q}^{00}$ is the unit matrix of order $10\times 10$; $\mathbf{E}^{00}$ and $\mathbf{H}^{00}$ are the vectors of homogeneous states of assumed strains and stress resultants; $\mathbf{E}^{01}$, $\mathbf{E}^{10}$, $\mathbf{E}^{11}$ and $\mathbf{H}^{01}$, $\mathbf{H}^{10}$, $\mathbf{H}^{11}$ are the vectors of higher approximation modes.

Substituting approximations (52), (53), (55) and (57) into the mixed variational equation (46) and integrating *analytically* throughout the element, one obtains governing equations of the developed finite element formulation

$$\mathbf{E}^{r_1r_2} = (\mathbf{Q}^{r_1\,r_2})^{\mathrm{T}} (\mathbf{B}^{r_1r_2} + \mathbf{R}^{r_1r_2}\mathbf{U})\,\mathbf{U}$$

$$\mathbf{H}^{r_1r_2} = (\mathbf{Q}^{r_1r_2})^{\mathrm{T}}\,\mathbf{D}\mathbf{Q}^{r_1r_2}\mathbf{E}^{r_1r_2}$$

$$\sum_{r_1,r_2} \frac{1}{3^{r_1+r_2}} (\mathbf{B}^{r_1r_2} + 2\mathbf{R}^{r_1r_2}\mathbf{U})^{\mathrm{T}}\mathbf{Q}^{r_1r_2}\mathbf{H}^{r_1r_2} = \mathbf{F} \tag{58}$$

where $\mathbf{F}$ is the element-wise surface force vector; $\mathbf{R}^{r_1r_2}$ are the 3D arrays of order $10\times 28\times 28$ defined as

$$\mathbf{R}^{00} = \mathbf{A}^{00} + \frac{1}{3}\mathbf{A}^{02} + \frac{1}{3}\mathbf{A}^{20} + \frac{1}{9}\mathbf{A}^{22}$$

$$\mathbf{R}^{10} = \mathbf{A}^{10} + \frac{1}{3}\mathbf{A}^{12}$$

$$\mathbf{R}^{01} = \mathbf{A}^{01} + \frac{1}{3}\mathbf{A}^{21}, \quad \mathbf{R}^{11} = \mathbf{A}^{11} \tag{59}$$

It should be noticed that during the analytical integration, we have supposed that a product $\sqrt{a}\Lambda$ is constant inside the element and according to Eq. B5 equals $(\sqrt{a}\Lambda)^{00}$.

It is important that the described non-linear geometrically exact four-node solid-shell element is too stiff in the case of using *coarse meshes* and some additional numerical procedure needs to be applied. The best solution of the problem is to employ the modified ANS method [Kulikov and Plotnikova (2007)]. The main idea of such approach can be traced back to the ANS method developed by Hughes and Tezduyar (1981) and Bathe and Dvorkin (1986). In contrast with this finite element formulation, we treat the term "ANS method" in a broader sense. In our formulation all in-plane and transverse components of the Green-Lagrange strain tensor in $(\xi^1, \xi^2, \xi^3)$-space are assumed to vary bilinearly inside the element. This implies that instead of the expected biquadratic interpolation (53) the more suitable ANS interpolation has to be used.

So, to improve a geometrically non-linear response of the shell, we interpolate the displacement-dependent strains inside the element as follows:

$$\boldsymbol{\varepsilon}^{\mathrm{ANS}} = \sum_r N_r \boldsymbol{\varepsilon}_r \tag{60}$$

where $\boldsymbol{\varepsilon}_r$ are the strain vectors of the element nodes whose components can be calculated in accordance with Appendix B. However, it is more convenient to rewrite the proposed strain interpolation (60) with the help of Eq. 53 in the following form:

$$\begin{aligned}\boldsymbol{\varepsilon}^{\mathrm{ANS}} &= \boldsymbol{\varepsilon}^{00} + \boldsymbol{\varepsilon}^{02} + \boldsymbol{\varepsilon}^{20} + \boldsymbol{\varepsilon}^{22} \\ &+ \xi^1\left(\boldsymbol{\varepsilon}^{10} + \boldsymbol{\varepsilon}^{12}\right) + \xi^2\left(\boldsymbol{\varepsilon}^{01} + \boldsymbol{\varepsilon}^{21}\right) \\ &+ \xi^1\xi^2\boldsymbol{\varepsilon}^{11}\end{aligned} \tag{61}$$

Substituting approximations (52), (57) and (61) into the variational equation (46), allowing for Eq. 55 and integrating *analytically*, one derives finite element equations (58), where instead of 3D arrays (59) the following 3D arrays should be used:

$$\mathbf{R}^{00} = \mathbf{A}^{00} + \mathbf{A}^{02} + \mathbf{A}^{20} + \mathbf{A}^{22}, \quad \mathbf{R}^{10} = \mathbf{A}^{10} + \mathbf{A}^{12}$$

$$\mathbf{R}^{01} = \mathbf{A}^{01} + \mathbf{A}^{21}, \quad \mathbf{R}^{11} = \mathbf{A}^{11} \tag{62}$$

Comparing Eqs. 59 and 62, one can observe that all corresponding arrays differ in multipliers 1/3 and 1/9. Therefore, no complication is involved into the finite element formulation employing the modified ANS method.

## 7 Incremental total Lagrangian formulation

Up to this moment, no incremental arguments are needed in the total Lagrangian formulation. The incremental displacements, strains and stress resultants are needed for solving non-linear equations (58) on the basis of the Newton-Raphson method. Further, the left superscripts $t$ and $t+\Delta t$ indicate in which configuration at time $t$ or time $t+\Delta t$ a quantity occurs. Then, in accordance with this agreement we have

$$\begin{aligned}{}^{t+\Delta t}\mathbf{U} &= {}^{t}\mathbf{U} + \Delta\mathbf{U} \\ {}^{t+\Delta t}\mathbf{F} &= {}^{t}\mathbf{F} + \Delta\mathbf{F} \\ {}^{t+\Delta t}\mathbf{E}^{r_1 r_2} &= {}^{t}\mathbf{E}^{r_1 r_2} + \Delta\mathbf{E}^{r_1 r_2} \\ {}^{t+\Delta t}\mathbf{H}^{r_1 r_2} &= {}^{t}\mathbf{H}^{r_1 r_2} + \Delta\mathbf{H}^{r_1 r_2}\end{aligned} \tag{63}$$

where $\Delta\mathbf{U}$, $\Delta\mathbf{F}$, $\Delta\mathbf{E}^{r_1 r_2}$ and $\Delta\mathbf{H}^{r_1 r_2}$ are the incremental variables.

Substituting relations (63) into governing equations (58) and taking into account the fact that external loads and second Piola-Kirchhoff stresses constitute the self-equilibrated system in a configuration at time $t$, one can obtain the incremental equations

$$\Delta\mathbf{E}^{r_1 r_2} = \left(\mathbf{Q}^{r_1 r_2}\right)^{\mathrm{T}}\left({}^{t}\mathbf{M}^{r_1 r_2} + \mathbf{R}^{r_1 r_2}\Delta\mathbf{U}\right)\Delta\mathbf{U}$$

$$\Delta\mathbf{H}^{r_1 r_2} = \overline{\mathbf{D}}^{r_1 r_2}\Delta\mathbf{E}^{r_1 r_2}$$

$$\begin{aligned}\sum_{r_1, r_2} \frac{1}{3^{r_1+r_2}} \Big[ & 2\left(\mathbf{R}^{r_1 r_2}\Delta\mathbf{U}\right)^{\mathrm{T}}\mathbf{Q}^{r_1 r_2}\,{}^{t}\mathbf{H}^{r_1 r_2} \\ & + \left({}^{t}\mathbf{M}^{r_1 r_2} + 2\mathbf{R}^{r_1 r_2}\Delta\mathbf{U}\right)^{\mathrm{T}}\mathbf{Q}^{r_1 r_2}\Delta\mathbf{H}^{r_1 r_2}\Big] = \Delta\mathbf{F}\end{aligned} \tag{64}$$

where

$$\begin{aligned}\overline{\mathbf{D}}^{r_1 r_2} &= \left(\mathbf{Q}^{r_1 r_2}\right)^{\mathrm{T}}\mathbf{D}\mathbf{Q}^{r_1 r_2} \\ {}^{t}\mathbf{M}^{r_1 r_2} &= \mathbf{B}^{r_1 r_2} + 2\mathbf{R}^{r_1 r_2}\,{}^{t}\mathbf{U}\end{aligned} \tag{65}$$

Due to existence of non-linear terms in incremental equations (64), the Newton-Raphson iteration process should be employed

$$\Delta\mathbf{U}^{[n+1]} = \Delta\mathbf{U}^{[n]} + \Delta\hat{\mathbf{U}}^{[n]},$$
$$\Delta\mathbf{E}^{r_1 r_2[n+1]} = \Delta\mathbf{E}^{r_1 r_2[n]} + \Delta\hat{\mathbf{E}}^{r_1 r_2[n]}$$
$$\Delta\mathbf{H}^{r_1 r_2[n+1]} = \Delta\mathbf{H}^{r_1 r_2[n]} + \Delta\hat{\mathbf{H}}^{r_1 r_2[n]}$$
$$\text{for } n = 0, 1, \ldots \quad (66)$$

As a result, we have

$$\Delta hat\mathbf{E}^{r_1 r_2[n]} - (\mathbf{Q}^{r_1 r_2})^{\mathrm{T}}\, {}^t\mathbf{L}^{r_1 r_2[n]}\Delta\hat{\mathbf{U}}^{[n]} = (\mathbf{Q}^{r_1 r_2})^{\mathrm{T}}\left({}^t\mathbf{L}^{r_1 r_2[n]} - \mathbf{R}^{r_1 r_2}\Delta\mathbf{U}^{[n]}\right)\Delta\mathbf{U}^{[n]} - \Delta\mathbf{E}^{r_1 r_2[n]} \quad (67)$$

$$\Delta\mathbf{H}^{r_1 r_2[n]} - \overline{D}^{r_1 r_2}\Delta\boldsymbol{\varepsilon}^{r_1 r_2[n]} = \overline{D}^{r_1 r_2}\Delta\mathbf{E}^{r_1 r_2[n]}$$

$$\sum_{r_1, r_2}\frac{1}{3^{r_1+r_2}}\left[2\left(\mathbf{R}^{r_1 r_2}\Delta\mathbf{Y}^{[n]}\right)^{\mathrm{T}}\mathbf{Q}^{r_1 r_2}\left({}^t\mathbf{H}^{r_1 r_2} + \Delta\mathbf{H}^{r_1 r_2[n]}\right) + \left({}^t\mathbf{L}^{r_1 r_2[n]}\right)^{\mathrm{T}}\mathbf{Q}^{r_1 r_2}\Delta\mathbf{H}^{r_1 r_2[n]}\right]$$
$$= \Delta\mathbf{F} - \sum_{r_1, r_2}\frac{1}{3^{r_1+r_2}}\left[2\left(\mathbf{R}^{r_1 r_2}\Delta\mathbf{U}^{[n]}\right)^{\mathrm{T}}\mathbf{Q}^{r_1 r_2 t}\mathbf{H}^{r_1 r_2} + \left({}^t\mathbf{L}^{r_1 r_2[n]}\right)^{\mathrm{T}}\mathbf{Q}^{r_1 r_2}\Delta\mathbf{H}^{r_1 r_2[n]}\right]$$

where

$$\mathbf{D}^{r_1 r_2} = \mathbf{Q}^{r_1 r_2}\overline{\mathbf{D}}^{r_1 r_2}\left(\mathbf{Q}^{r_1 r_2}\right)^{\mathrm{T}}$$
$${}^t\mathbf{L}^{r_1 r_2[n]} = \mathbf{B}^{r_1 r_2} + 2\mathbf{R}^{r_1 r_2}\left({}^t\mathbf{U} + \Delta\mathbf{U}^{[n]}\right) \quad (68)$$

Eliminating incremental strains $\Delta\hat{\mathbf{E}}^{r_1 r_2[n]}$ and stress resultants $\Delta\hat{\mathbf{H}}^{r_1 r_2[n]}$ from Eq. 67 and taking into account the matrix transformation (C3) from Appendix C, one derives a system of linearized equilibrium equations

$$\mathbf{K}\Delta\hat{\mathbf{U}}^{[n]} = \Delta\hat{\mathbf{F}}^{[n]} \quad (69)$$

where

$$\Delta\hat{\mathbf{F}}^{[n]} = \Delta\mathbf{F} - \sum_{r_1, r_2}\frac{1}{3^{r_1+r_2}}\left[\left({}^t\mathbf{L}^{r_1 r_2[n]}\right)^{\mathrm{T}}\mathbf{D}^{r_1 r_2}\left({}^t\mathbf{L}^{r_1 r_2[n]} - \mathbf{R}^{r_1 r_2}\Delta\mathbf{U}^{[n]}\right) + 2\left(\mathbf{Q}^{r_1 r_2 t}\mathbf{H}^{r_1 r_2}\right)\mathbf{R}^{r_1 r_2}\right]\Delta\mathbf{U}^{[n]} \quad (70)$$

and $\mathbf{K} = \mathbf{K}_{\mathrm{D}} + \mathbf{K}_{\mathrm{H}}$ denotes the elemental stiffness matrix defined as

$$\mathbf{K}_{\mathrm{D}} = \sum_{r_1, r_2}\frac{1}{3^{r_1+r_2}}\left({}^t\mathbf{L}^{r_1 r_2[n]}\right)^{\mathrm{T}}\mathbf{D}^{r_1 r_2 t}\mathbf{L}^{r_1 r_2[n]}$$

$$\mathbf{K}_{\mathrm{H}} = 2\sum_{r_1, r_2}\frac{1}{3^{r_1+r_2}}\left(\mathbf{Q}^{r_1 r_2 t}\mathbf{H}^{r_1 r_2} + \underline{\mathbf{Q}^{r_1 r_2}\Delta\mathbf{H}^{r_1 r_2[n]}}\right)\mathbf{R}^{r_1 r_2} \quad (71)$$

As expected, the tangent stiffness matrix $\mathbf{K}$ is symmetric [see discussion on this subject in a paper of Suetake, Iura and Atluri (2003)]. This is due to the fact that both matrices $\mathbf{K}_{\mathrm{D}}$ and $\mathbf{K}_{\mathrm{H}}$ are symmetric. The proof of symmetry of the second matrix can be found in Appendix C.

Finally, we represent a formula that is used in Eq. 71 for computation of incremental stress resultant vectors at the $n$th iteration step

$$\mathbf{Q}^{r_1 r_2}\Delta\mathbf{H}^{r_1 r_2[n]} = \mathbf{D}^{r_1 r_2}\left[\left({}^t\mathbf{M}^{r_1 r_2} + 2\mathbf{R}^{r_1 r_2}\Delta\mathbf{U}^{[n-1]}\right)\Delta\mathbf{U}^{[n]} - \left(\mathbf{R}^{r_1 r_2}\Delta\mathbf{U}^{[n-1]}\right)\Delta\mathbf{U}^{[n-1]}\right] \quad (72)$$

This formula holds for $n \geq 1$, whereas at the beginning of each iteration process one should set

$$\Delta\mathbf{U}^{[0]} = \mathbf{0} \quad \text{and} \quad \Delta\mathbf{H}^{r_1 r_2[0]} = \mathbf{0} \quad (73)$$

**Remark 4.** The proposed incremental approach allows one to utilize load increments, which are much larger than possible with the standard geometrically exact shell element formulation [Kulikov and Plotnikova (2006)]. This is because of the fact that an additional load vector due to so-called compatibility mismatch [Atluri (1973), Boland and Pian (1977), Cho and Lee (1996)] is present in linearized equilibrium equations (69) and disappears only at the end of the iteration process.

**Remark 5.** The tangent stiffness matrix possesses a correct rank because 22 assumed strain parameters are accepted according to Eq. 57a. It is worth noting that both elemental matrices (71) require only direct substitutions, i.e., no inversion is needed to derive them. Furthermore, our stiffness matrix is evaluated by using the analytical integration.

The equilibrium equations (69)-(71) for each element are assembled by the usual technique to form the global incremental equilibrium equations. These incremental equations should be performed until the required accuracy of the solution can be obtained. Herein, two convergence criteria are employed to describe more carefully high potential of the proposed finite element formulation, namely,

$$\left\| \Delta \mathbf{U}_G^{[n+1]} - \Delta \mathbf{U}_G^{[n]} \right\| < \varepsilon \left\| \Delta \mathbf{U}_G^{[n]} \right\| \tag{74}$$

and

$$\left| W^{[n+1]} - W^{[n]} \right| < \varepsilon \left| W^{[n]} \right| \tag{75}$$

where $\|\cdot\|$ stands for the Euclidean norm; $\Delta\mathbf{U}_G$ is the global vector of displacement increments; $W$ is the strain energy; $\varepsilon$ is the prescribed tolerance.

## 8 Benchmark problems

The performance of the proposed geometrically exact four-node solid-shell element is evaluated by comparing with the best solid-shell elements extracted from the literature. A listing of these elements and the abbreviations used to identify them are contained in Table I. All our results are compared with those based, as a rule, on using identical node spacing and the same convergence criterion and tolerance. In each numerical example, NStep denotes the number of load steps employed to *equally* divide the maximum load, whereas NIter stands for the total number of iterations. Note also that all computations were performed on a standard PC Pentium IV using Delphi environment.

### *8.1 Cantilever curved beam*

Consider first a geometrically linear thick cantilever curved beam whose centerline is one quarter of the circle. The beam of the unit width is subjected to the shear tip load as shown in Figure 7. Figure 8 displays results of solving the elasticity problem [Atluri, Liu and Han (2006a) and (2006b)] using the MLPG method with 25 nodes in the $\theta$-direction and 5 nodes in the thickness direction. Thus, we have taken the same number of equally located nodes. The centerline displacements in $x$- and $y$-directions are normalized with respect to the values of $u_x^c(0) = -502.23$ and $u_y^c(0) = -321.10$. These values are provided by the exact solution of the plane stress problem in Timoshenko and Goodier (1970). One can see that the proposed 7-parameter model describes a behavior of the thick curved beam well.

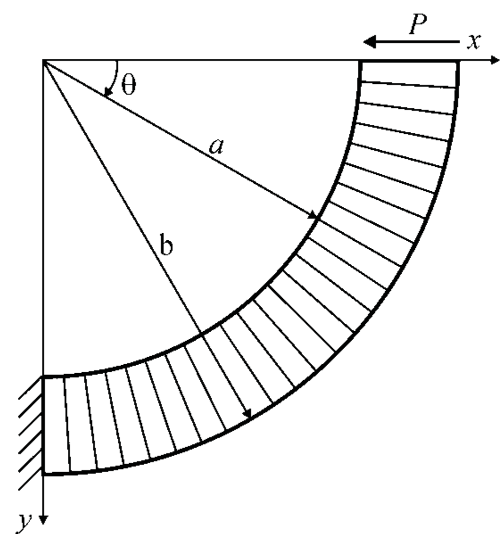


Figure 7: Cantilever curved beam under the shear tip load with $a = 13$, $b = 17$, $E = 1$, $\nu = 0.25$, $P = 1$

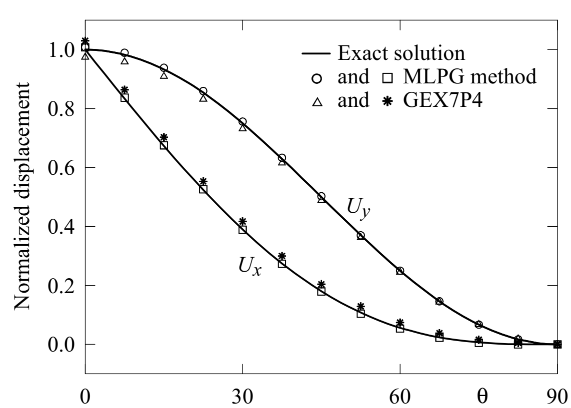


Figure 8: Normalized centerline displacements in $x$- and $y$-directions of the curved beam

Table 1: Listing of non-linear solid-shell elements

| Name | Description |
|---|---|
| GEX7P4 | Geometrically exact assumed stress-strain four-node element developed on the basis of the seven-parameter shell formulation |
| GEX6P4 | Geometrically exact assumed stress-strain four-node element on the basis of the six-parameter shell formulation [Kulikov and Plotnikova (2007)] |
| ISO6P4 | Isoparametric assumed stress four-node element on the basis of the six-parameter shell formulation [Sze, Chan and Pian (2002)] |
| ISO6P8 | Isoparametric displacement-based eight-node element on the basis of the six-parameter shell formulation in conjunction with the enhanced assumed strain concept [Braun, Bischoff and Ramm (1994)] |
| ISO6P9 | Isoparametric assumed strain nine-node element on the basis of the six-parameter shell formulation [Park, Cho and Lee (1995)] |
| S4R | Isoparametric displacement-based four-node element with reduced integration and hourglass control [ABAQUS (1998)] |

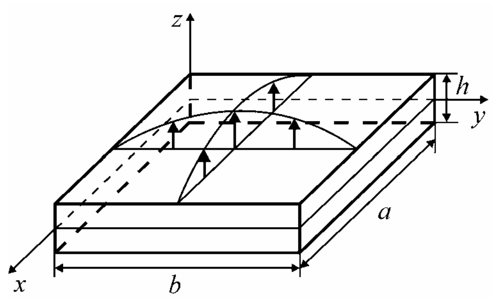


$a = b$, $E_L = 2.5\times10^7$, $E_T = 10^6$, $G_{LT} = 5\times10^5$
$G_{TT} = 2\times10^5$, $\nu_{LT} = \nu_{TT} = 0.25$
Ply orientation $= [0/90]$, Ply thickness $= \left[\frac{1}{2}h/\frac{1}{2}h\right]$

Figure 9: Rectangular two-layer cross-ply plate

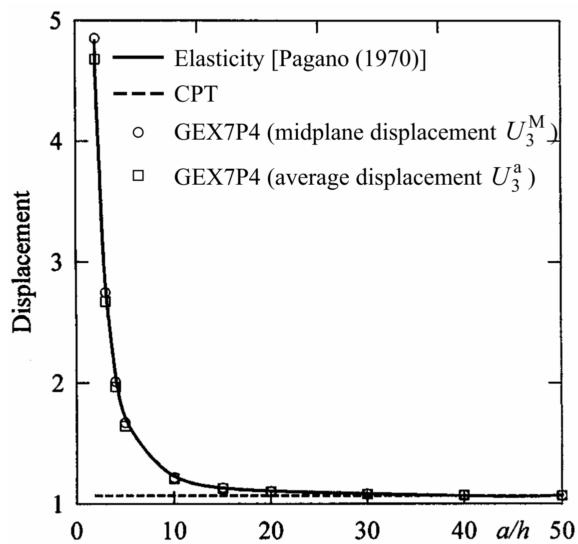


Figure 10: Transverse displacement at the center point $U_3 = 100E_T h^3 u_3/p_0 a^4$ of the rectangular two-layer cross-ply plate

### *8.2 Rectangular cross-ply plate*

Next, we study a linear rectangular two-layer cross-ply simply supported plate subjected to the sinusoidally distributed pressure load. The geometrical and material characteristics of the plate are given in Figure 9. Due to symmetry of the problem, only one quarter of the plate is modeled by $32\times32$ mesh of GEX7P4 elements. A comparison with analytical solutions based on the elasticity theory [Pagano (1970)] and classical plate theory (CPT) as well is given in Figure 10. As can be seen, the average transverse displacement at the center point $u_3^{\mathrm{a}} = \left(u_3^- + u_3^+\right)/2$ practically coincides with the midplane displacement $u_3^{\mathrm{M}}$ in a range of $a/h \geq 10$.

### *8.3 Pinched hemispherical shell*

To investigate the capability of the proposed geometrically exact shell element to model the inextensional bending and large rigid-body motions, we consider one of the most demanding nonlinear tests. A hemispherical shell with $18^o$ hole at the top is loaded by two pairs of opposite forces on the equator. The geometrical and material data of the problem are shown in Figure 11. Owing to symmetry, only one quarter of the shell is modeled with regular meshes of GEX7P4 elements. Table 2 lists midsurface displacements under applied loads employing geometrically exact and isoparametric solid-shell elements from Table 1. One can observe that the GEX7P4 element is a bit stiff comparing to the GEX6P4 element because of utilizing the complete 3D constitutive equations. At the same time it performs excellently for coarse meshes. For example, a very coarse mesh $4 \times 4$ yields 86 % of the reference displacement value at point A provided by ABAQUS's S4R element [Sze, Liu and Lo (2004)].

The data in Table 3 exhibit monotonic convergence of the Newton-Raphson iteration scheme through the Euclidean norm of the displacement vector and the energy variation as well. For a complete picture Figure 12 presents load-displacement curves compared with those derived by a $16 \times 16$ mesh of S4R elements. It is seen that all results agree closely but the GEX7P4 element is less expensive owing to the economical derivation of its stiffness matrix.

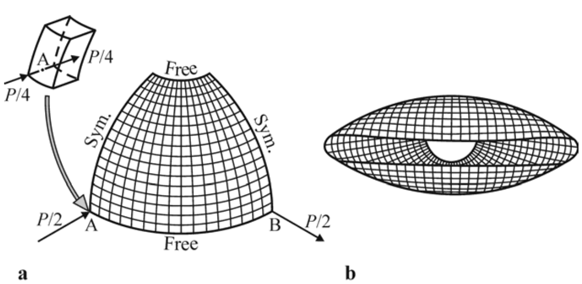


$R$=10, $h$=0.04, Hole=18°, $E$=6.825×10^7, ν=0.3, $P$=100$f$, $f$=4

Figure 11: Pinched hemispherical shell: (a) geometry and (b) deformed configuration (modeled by $16 \times 16$ mesh)

## 8.4 Slit ring plate under line load

This example is considered in the literature to test non-linear finite element formulations for thin-walled shell structures and has been extensively used by many investigators. The ring plate is subjected to a line load $P$ applied at its free edge of the slit, while the other edge is fully clamped (Fig-

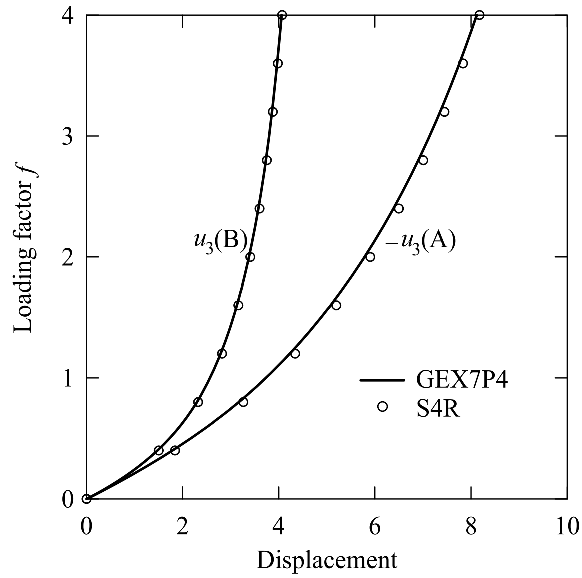


Figure 12: Midsurface displacements of the pinched hemispherical shell (modeled by $16 \times 16$ mesh)

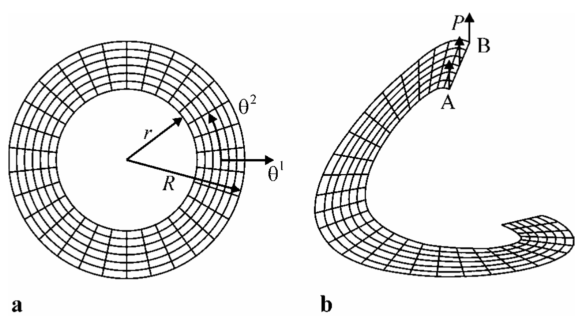


$r$=6, $R$=10, $h$=0.03, $E$=2.1×10^7, ν=0, $P$=0.8

Figure 13: Slit ring plate under the line load: (a) geometry and (b) deformed configuration (modeled by $6 \times 30$ mesh)

ure 13). The plate is modeled by a shell of revolution with geometrical parameters

$$A_1 = 1,\ A_2 = r + \theta^1,\ k_1 = k_2 = 0,$$
$$\theta^1 \in [0,\ R - r],\ \theta^2 \in [0,\ 2\pi]. \quad (76)$$

The displacements at points A and B of the plate, presented in Table 4 and Figure 14, have been found by employing uniform meshes of geometrically exact elements. A comparison with ABAQUS's S4R element [Sze, Liu and Lo

Table 2: Midsurface displacements at points A and B of the pinched hemispherical shell using displacement-based criterion (74) with tolerance of $10^{-4}$

| Output | GEX7P4 $4\times4$mesh | GEX7P4 $8\times8$mesh | GEX7P4 $16\times16$mesh | GEX6P4 $16\times16$mesh | S4R $16\times16$mesh | ISO6P4 $16\times16$mesh | ISO6P9 $8\times8$mesh |
|---|---|---|---|---|---|---|---|
| $u_3$ (B) | 3.2631 | 3.9536 | 4.0545 | 4.0557 | 4.067 | 4.0488 | 4.0205 |
| $-u_3$ (A) | 7.0379 | 8.0897 | 8.1232 | 8.1451 | 8.178 | 8.1173 | 8.0160 |
| NStep/NIter | 1/7 | 1/7 | 1/7 | 1/7 | 40/136[a] | 1/8 | 1/8 |

[a] NIter = 136 in case of using 27 *non-uniform* load increments [Sze, Liu and Lo (2004)]

Table 3: Convergence results for the pinched hemispherical shell employing a $16\times16$ mesh of GEX7P4 elements when the total load $P = 400$ is applied in one load step

| Iteration | $\left\Vert \mathbf{U}_G^{[n+1]} - \mathbf{U}_G^{[n]} \right\Vert$ | $\left\vert W^{[n+1]} - W^{[n]} \right\vert$ |
|---|---|---|
| 0 | $2.1276E+2$ | $3.6824E+3$ |
| 1 | $9.8503E+1$ | $2.7725E+8$ |
| 2 | $3.8491E+1$ | $2.6215E+8$ |
| 3 | $1.0859E+1$ | $1.3956E+7$ |
| 4 | $2.5914E+0$ | $1.1426E+6$ |
| 5 | $7.3852E-1$ | $8.0632E+3$ |
| 6 | $1.4760E-2$ | $2.1392E+0$ |
| 7 | $3.4456E-6$ | $1.9763E-5$ |
| 8 | $3.2743E-11$ | $5.2989E-9$ |

Table 4: Midplane displacements at points A and B of the slit ring plate using displacement-based criterion (74) with tolerance of $10^{-4}$

| Output | GEX7P4 $2\times4$mesh | GEX7P4 $4\times8$mesh | GEX7P4 $16\times32$mesh | GEX7P4 $10\times80$mesh | GEX6P4 $10\times80$mesh | S4R $10\times80$mesh |
|---|---|---|---|---|---|---|
| $u_3$ (A) | 12.742 | 12.578 | 13.670 | 13.765 | 13.760 | 13.891 |
| $u_3$ (B) | 16.029 | 16.096 | 17.307 | 17.402 | 17.398 | 17.528 |
| NStep/NIter | 1/6 | 1/7 | 1/10 | 1/13 | 1/12 | 640/346[a] |

[a] NIter = 346 in case of using 67 *non-uniform* load increments [Sze, Liu and Lo (2004)]

(2004)] is also given. As can be seen, extremely coarse meshes with the GEX7P4 element can be used because the $2\times4$ mesh already yields 91 % of the reference solution provided by a S4R element. Note also that in this case only 6 Newton iterations are needed to find a converged solution with the chosen criterion and tolerance.

### 8.5 *Pinched three-layer hyperbolic shell*

Further, we consider cross-ply and angle-ply hyperbolic shells under two pairs of opposite forces. The geometrical and material data of the three-layer hyperbolic shell are shown in Figure 15. This shell of revolution is characterized by the following geometrical parameters:

$$A_1 = \sqrt{1+\frac{\mu^2 z^2}{A_2^2}}, \quad A_2 = r\sqrt{1+\frac{\mu z^2}{r^2}}$$

$$k_1 = -\frac{\mu r^2}{A_1^3 A_2^3}, \quad k_2 = \frac{1}{A_1 A_2}, \quad \mu = \frac{R^2-r^2}{L^2}$$

where $\theta^1 = z \in [-L,\, L]$ and $\theta^2 \in [0,\, 2\pi]$ denote meridional and circumferential midsurface coordinates. Two cross-ply hyperbolic shells with different ply orientations of [0/90/0] and [90/0/90], but the same ply thickness of $\left[\frac{1}{3}h/\frac{1}{3}h/\frac{1}{3}h\right]$ are investigated, where 0° and 90° refer to the circumferential and meridional directions. Additionally, we study an angle-ply hyperbolic shell with

Table 5: Midsurface displacements at points A and C of the pinched three-layer hyperbolic shell using displacement-based criterion (74) with tolerance of $10^{-4}$

| Ply orientation = [0/90/0] | | | | | |
|---|---|---|---|---|---|
| Output | GEX7P4 $4\times4$mesh | GEX7P4 $8\times8$mesh | GEX7P4 $16\times16$mesh | GEX7P4 $32\times32$mesh | GEX6P4 $32\times32$mesh |
| $-u_y$(A) | 2.5940 | 3.3076 | 3.4732 | 3.5217 | 3.5215 |
| $u_y$(C) | 2.2453 | 2.5210 | 2.5224 | 2.5185 | 2.5179 |
| NStep/NIter | 1/7 | 1/7 | 1/7 | 1/7 | 1/8 |
| Ply orientation = [90/0/90] | | | | | |
| Output | GEX7P4 $4\times4$mesh | GEX7P4 $8\times8$mesh | GEX7P4 $16\times16$mesh | GEX7P4 $32\times32$mesh | GEX6P4 $32\times32$mesh |
| $-u_y$(A) | 3.0685 | 4.7555 | 5.6299 | 6.1294 | 6.1330 |
| $u_y$(C) | 2.5310 | 2.9118 | 2.8972 | 2.6932 | 2.6914 |
| NStep/NIter | 1/10 | 2/16 | 2/20 | 5/25 | 5/29 |
| Ply orientation = $[\gamma/-\gamma/\gamma]$ | | | | | |
| Output | GEX7P4 $4\times16$mesh | GEX7P4 $8\times32$mesh | GEX7P4 $16\times64$mesh | GEX7P4 $32\times128$mesh | GEX6P4 $32\times128$mesh |
| $-u_y$(A) | 3.0426 | 4.8838 | 5.7172 | 5.9587 | 5.9566 |
| $u_y$(C) | 2.5013 | 2.8945 | 2.8038 | 2.7063 | 2.7080 |
| NStep/NIter | 2/12 | 4/18 | 4/18 | 4/22 | 4/25 |

[a] Results have been found by using a GEX6P4 element and are published for the first time

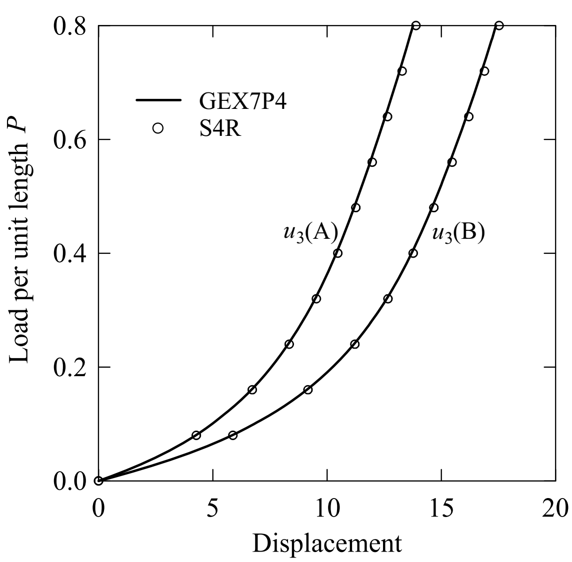


Figure 14: Midplane displacements of the slit ring plate (modeled by $10\times80$ mesh)

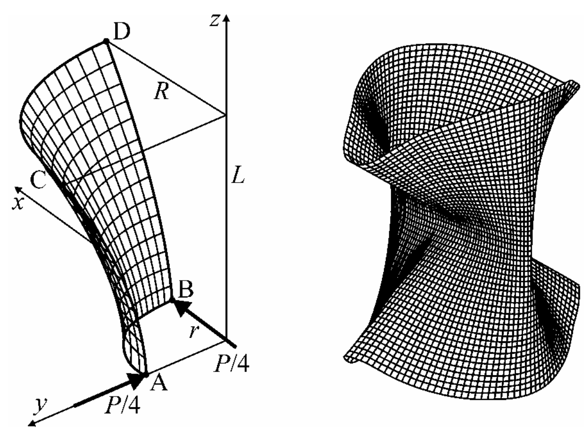


Figure 15: Pinched three-layer hyperbolic shell: geometry and deformed configuration for the ply orientation [90/0/90] (modeled by $28\times28$ mesh) with $r=7.5$, $R=15$, $L=20$, $h=0.04$, $E_L=4\times10^7$, $E_T=10^6$, $G_{LT}=G_{TT}=6\times10^5$, $\nu_{LT}=\nu_{TT}=0.25$, $P=80f$, $f=5$

$[\gamma/-\gamma/\gamma]$ and $\left[\frac{1}{4}h/\frac{1}{2}h/\frac{1}{4}h\right]$, where $\gamma$ is the angle between the asymptotic line of the midsurface and the tangent to the meridian measured in the clockwise direction. This angle can be found by a simple formula

$$\cos\gamma = \frac{A_1}{\sqrt{1+\mu}}$$

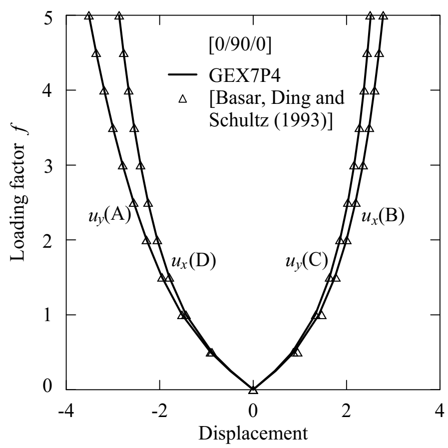


(a)

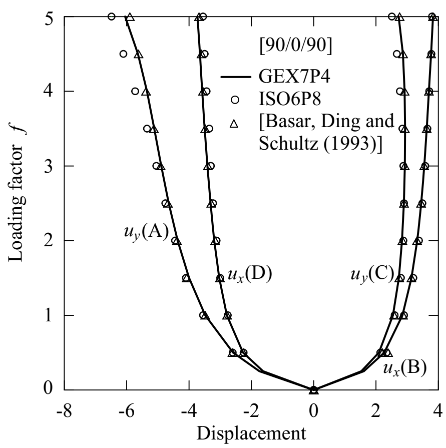


(b)

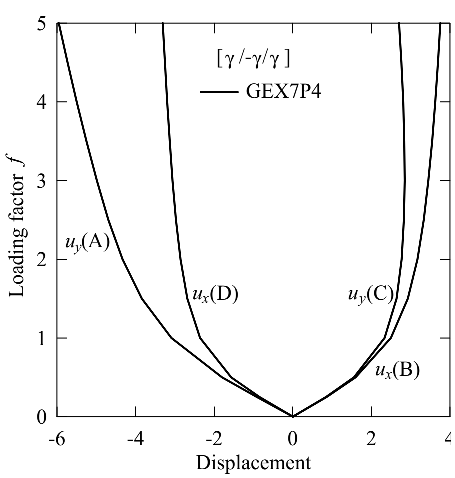


(c)

Figure 16: Midsurface displacements of the pinched three-layer hyperbolic shell for ply orientations: (a) [0/90/0] and (b) [90/0/90] (modeled by $28 \times 28$ mesh), and (c) $[\gamma/-\gamma/\gamma]$ (modeled by $32 \times 128$ mesh)

Due to symmetry of the problem, only one octant of the cross-ply shell and one half of the angle-ply shell are discretized with uniform meshes. Table 5 and Figure 16 present displacements derived by using geometrically exact elements for all ply sequences, where $u_x$ and $u_y$ denote displacements of the midsurface in $x$- and $y$-directions. The results for cross-ply configurations are compared with those obtained by Basar, Ding and Schultz (1993), and Braun, Bischoff and Ramm (1994) employing the $28 \times 28$ mesh of bilinear degenerated-shell and the $14 \times 14$ mesh of quadratic solid-shell elements, respectively. One can observe that the GEX7P4 element performs excellently because only one load step and 7 Newton iterations are needed to derive a converged solution for the [0/90/0] ply orientation. Unfortunately, we have no possibility to compare these results with those based on the isoparametric finite element formulation because in the above papers, a convergence criterion and load increments are not mentioned.

## 9 Conclusions

The simple and efficient geometrically exact assumed stress-strain four-node solid-shell element GEX7P4 has been developed for analyses of homogeneous and multilayered composite shells undergoing finite rotations. The finite element formulation is based on the non-linear strain-displacement relationships, which are invariant under arbitrarily large rigid-body shell motions in convected curvilinear coordinate system. This is due to our approach in which the displacement vectors of outer and middle surfaces are introduced and resolved in the reference surface frame. The proposed geometrically exact solid-shell element model is free of assumptions of small displacements, small rotations and small loading steps because it is based on the objective fully non-linear strain-displacement relationships. This model is robust because it allows us, first, to use much larger load increments than existing geometrically exact shell element models and, second, to utilize the complete 3D constitutive equations.

The tangent stiffness matrix developed does not require expensive numerical matrix inversions that is unusual for the isoparametric hybrid/mixed shell element formulations and it is evaluated by using the 3D analytical integration. It is noteworthy that the GEX7P4 element permits one to employ very coarse meshes even in shell problems with extremely large displacements and rotations, and it is *insensitive* to the number of load increments.

**Acknowledgement:** The support of this work by Russian Foundation for Basic Research (RFBR) under Grant No 08-01-00373 is gratefully acknowledged.

## Appendix A Strain-Displacement Relationships in Orthogonal Curvilinear Coordinate System

Herein, we briefly summarize the strain-displacement relationships for one particular case. If the orthogonal curvilinear coordinates are referred to the lines of principal curvatures of the reference surface $\Omega$, then

$$\begin{aligned} &\mathbf{a}_\alpha = A_\alpha \mathbf{e}_\alpha, \quad \mathbf{a}_3 = \mathbf{e}_3 \\ &b_1^1 = -k_1, \quad b_2^2 = -k_2, \quad b_1^2 = b_2^1 = 0 \end{aligned} \tag{A1}$$

where $\mathbf{e}_i$ are the orthonormal base vectors of the reference surface; $A_\alpha$ and $k_\alpha$ are the coefficients of the first fundamental form and principal curvatures of the reference surface. The use of Eq. A1 in Eqs. 6 and 8 leads to

$$\begin{aligned} &\mu_1^{I1} = c_1^I = 1 + k_1 z^I, \quad \mu_2^{I2} = c_2^I = 1 + k_2 z^I \\ &\mu_1^{I2} = \mu_2^{I1} = 0 \end{aligned} \tag{A2}$$

$$\mathbf{g}_\alpha^I = A_\alpha c_\alpha^I \mathbf{e}_\alpha, \quad \mathbf{g}_3^I = \mathbf{e}_3 \tag{A3}$$

From Eqs. 24 and A3 follow the needed strain-displacement relationships

$$\begin{aligned} 2\dot{\varepsilon}_{\alpha\beta}^I &= \frac{1}{A_\alpha} c_\beta^I \mathbf{u}_{,\alpha}^I \cdot \mathbf{e}_\beta + \frac{1}{A_\beta} c_\alpha^I \mathbf{u}_{,\beta}^I \cdot \mathbf{e}_\alpha \\ &\qquad + \frac{1}{A_\alpha A_\beta} \mathbf{u}_{,\alpha}^I \cdot \mathbf{u}_{,\beta}^I \\ 2\dot{\varepsilon}_{\alpha 3}^I &= c_\alpha^I \boldsymbol{\beta}^I \cdot \mathbf{e}_\alpha + \frac{1}{A_\alpha} \mathbf{u}_{,\alpha}^I \cdot \left(\mathbf{e}_3 + \boldsymbol{\beta}^I\right) \\ 2\dot{\varepsilon}_{33}^I &= \boldsymbol{\beta}^I \cdot \left(2\mathbf{e}_3 + \boldsymbol{\beta}^I\right) \end{aligned} \tag{A4}$$

where $\dot{\varepsilon}_{ij}^I$ are the components of the Green-Lagrange strain tensor at outer and middle surfaces in the orthonormal reference surface frame.

The displacement vectors and their derivatives with respect to coordinate $\theta^3$ at outer and middle surfaces can be represented in this orthonormal frame as follows:

$$\mathbf{u}^I = \sum_i \dot{u}_i^I \mathbf{e}_i \tag{A5}$$

$$\boldsymbol{\beta}^I = \sum_i \dot{\beta}_i^I \mathbf{e}_i \tag{A6}$$

Taking into account Eq. A5 and well-known formulas for the derivatives of orthonormal vectors $\mathbf{e}_i$ with respect to coordinates $\theta^\alpha$ [see e.g. Kulikov and Plotnikova (2007)], one derives

$$\frac{1}{A_\alpha} \mathbf{u}_{,\alpha}^I = \sum_i \lambda_{i\alpha}^I \mathbf{e}_i \tag{A7}$$

where

$$\lambda_{\alpha\alpha}^I = \left(\frac{1}{A_\alpha} \dot{u}_\alpha^I\right)_{,\alpha} + B_{\alpha\alpha} \dot{u}_\alpha^I + B_{\alpha\beta} \dot{u}_\beta^I + k_\alpha \dot{u}_3^I \quad \text{for } \beta \neq \alpha$$

$$\lambda_{\beta\alpha}^I = \left(\frac{1}{A_\alpha} \dot{u}_\beta^I\right)_{,\alpha} + B_{\alpha\alpha} \dot{u}_\beta^I - B_{\alpha\beta} \dot{u}_\alpha^I \quad \text{for } \beta \neq \alpha$$

$$\begin{aligned} &\lambda_{3\alpha}^I = \left(\frac{1}{A_\alpha} \dot{u}_3^I\right)_{,\alpha} + B_{\alpha\alpha} \dot{u}_3^I - k_\alpha \dot{u}_\alpha^I \\ &B_{\alpha\beta} = \frac{1}{A_\alpha A_\beta} A_{\alpha,\beta} \end{aligned} \tag{A8}$$

Substituting Eqs. A6 and A7 into Eq. A4, we arrive at the final strain-displacement relationships

$$\begin{aligned} 2\dot{\varepsilon}_{\alpha\beta}^I &= c_\alpha^I \lambda_{\alpha\beta}^I + c_\beta^I \lambda_{\beta\alpha}^I + \sum_i \lambda_{i\alpha}^I \lambda_{i\beta}^I \\ 2\dot{\varepsilon}_{\alpha 3}^I &= c_\alpha^I \dot{\beta}_\alpha^I + \lambda_{3\alpha}^I + \sum_i \dot{\beta}_i^I \lambda_{i\alpha}^I \\ 2\dot{\varepsilon}_{33}^I &= 2\dot{\beta}_3^I + \sum_i \dot{\beta}_i^I \dot{\beta}_i^I \end{aligned} \tag{A9}$$

It is worth noting that strain-displacement relationships A9 are also invariant under arbitrarily large rigid-body motions.

## Appendix B Evaluation of Mode Strain Vectors

As in Appendix A, we consider strain-displacement relationships in orthogonal curvilinear coordinates, which are referred to the lines of principal curvatures of the reference surface. Allowing for biquadratic interpolation (53) and strain-displacement relationships (40) and (A9), one finds

$$\dot{\varepsilon}_{\alpha\beta}^{As_1s_2} = e_{\alpha\beta}^{As_1s_2} + \eta_{\alpha\beta}^{As_1s_2}, \quad \dot{\varepsilon}_{33}^{As_1s_2} = e_{33}^{As_1s_2} + \eta_{33}^{As_1s_2}$$

$$\dot{\varepsilon}_{\alpha3}^{\mathrm{a}s_1s_2} = \frac{1}{2}\left(e_{\alpha3}^{-s_1s_2} + e_{\alpha3}^{+s_1s_2}\right) + \frac{1}{2}\left(\eta_{\alpha3}^{-s_1s_2} + \eta_{\alpha3}^{+s_1s_2}\right) \tag{B1}$$

where $e_{ij}^{As_1s_2}$ and $\eta_{ij}^{As_1s_2}$ are the linear and non-linear parts of mode Green-Lagrange strains of the bottom and top surfaces defined as

$$2e_{\alpha\beta}^{Ar_1r_2} = c_\alpha^{A00}\lambda_{\alpha\beta}^{Ar_1r_2} + c_\beta^{A00}\lambda_{\beta\alpha}^{Ar_1r_2}, \quad e_{33}^{Ar_1r_2} = \dot{\beta}_3^{Ar_1r_2}$$

$$2e_{\alpha3}^{Ar_1r_2} = c_\alpha^{A00}\dot{\beta}_\alpha^{Ar_1r_2} + \lambda_{3\alpha}^{Ar_1r_2}$$

$$e_{ij}^{As_1s_2} = 0 \text{ for } s_1 = 2 \text{ or } s_2 = 2 \tag{B2}$$

and

$$2\eta_{\alpha\beta}^{As_1s_2} = \sum_{\substack{r_1+r_3=s_1\\ r_2+r_4=s_2}} \left(\sum_i \lambda_{i\alpha}^{Ar_1r_2}\lambda_{i\beta}^{Ar_3r_4}\right)$$

$$2\eta_{\alpha3}^{As_1s_2} = \sum_{\substack{r_1+r_3=s_1\\ r_2+r_4=s_2}} \left(\sum_i \dot{\beta}_i^{Ar_1r_2}\lambda_{i\alpha}^{Ar_3r_4}\right)$$

$$2\eta_{33}^{As_1s_2} = \sum_{\substack{r_1+r_3=s_1\\ r_2+r_4=s_2}} \left(\sum_i \dot{\beta}_i^{Ar_1r_2}\dot{\beta}_i^{Ar_3r_4}\right) \tag{B3}$$

where according to Eq. 28 and A8 the following notations are introduced:

$$\lambda_{\alpha\alpha}^{Ar_1r_2} = \left\{\frac{1}{\tilde{A}_\alpha}\dot{u}_\alpha^A\right\}_\alpha^{r_1r_2} + \left(B_{\alpha\alpha}\dot{u}_\alpha^A + B_{\alpha\beta}\dot{u}_\beta^A + k_\alpha\dot{u}_3^A\right)^{r_1r_2} \quad \text{for } \beta \neq \alpha$$

$$\lambda_{\beta\alpha}^{Ar_1r_2} = \left\{\frac{1}{\tilde{A}_\alpha}\dot{u}_\beta^A\right\}_\alpha^{r_1r_2} + \left(B_{\alpha\alpha}\dot{u}_\beta^A - B_{\alpha\beta}\dot{u}_\alpha^A\right)^{r_1r_2} \quad \text{for } \beta \neq \alpha$$

$$\lambda_{3\alpha}^{Ar_1r_2} = \left\{\frac{1}{\tilde{A}_\alpha}\dot{u}_3^A\right\}_\alpha^{r_1r_2} + \left(B_{\alpha\alpha}\dot{u}_3^A - k_\alpha\dot{u}_\alpha^A\right)^{r_1r_2}$$

$$\dot{\beta}_i^{-r_1r_2} = \frac{1}{h}\left(-3\dot{u}_i^- + 4\dot{u}_i^{\mathrm{M}} - \dot{u}_i^+\right)^{r_1r_2}$$

$$\dot{\beta}_i^{+r_1r_2} = \frac{1}{h}\left(\dot{u}_i^- - 4\dot{u}_i^{\mathrm{M}} + 3\dot{u}_i^+\right)^{r_1r_2}$$

$$\tilde{A}_1 = \ell^1 A_1, \quad \tilde{A}_2 = \ell^2 A_2 \tag{B4}$$

Here, $\xi^\alpha = (\theta^\alpha - c^\alpha)/\ell^\alpha$ are the normalized curvilinear coordinates and, as we remember, the superscripts $r_1$, $r_2$, $r_3$ and $r_4$ run from 0 to 1, whereas the superscripts $s_1$ and $s_2$ run from 0 to 2. Note also that due to Eq. 52 and Figure B1 convenient mesh notations are employed

$$f^{00} = \frac{1}{4}\left[f\left(\tilde{P}_1\right) + f\left(\tilde{P}_2\right) + f\left(\tilde{P}_3\right) + f\left(\tilde{P}_4\right)\right]$$

$$f^{10} = \frac{1}{4}\left[f\left(\tilde{P}_1\right) - f\left(\tilde{P}_2\right) - f\left(\tilde{P}_3\right) + f\left(\tilde{P}_4\right)\right]$$

$$f^{01} = \frac{1}{4}\left[f\left(\tilde{P}_1\right) + f\left(\tilde{P}_2\right) - f\left(\tilde{P}_3\right) - f\left(\tilde{P}_4\right)\right]$$

$$f^{11} = \frac{1}{4}\left[f\left(\tilde{P}_1\right) - f\left(\tilde{P}_2\right) + f\left(\tilde{P}_3\right) - f\left(\tilde{P}_4\right)\right]$$

$$\{f\}_1^{00} = f^{10}, \quad \{f\}_1^{01} = f^{11}, \quad \{f\}_1^{10} = \{f\}_1^{11} = 0$$

$$\{f\}_2^{00} = f^{01}, \quad \{f\}_2^{10} = f^{11}, \quad \{f\}_2^{01} = \{f\}_2^{11} = 0 \tag{B5}$$

where $f\left(\xi^1, \xi^2\right)$ is any function; $\tilde{P}_r$ are the nodal points of the element and derivatives from Eq. A8 are evaluated by means of a simple scheme as

$$\frac{\partial}{\partial\xi^1}\left(\frac{1}{\tilde{A}_1}\dot{u}_i^A\right) = \left(\frac{1}{\tilde{A}_1}\dot{u}_i^A\right)^{10} + \xi^2\left(\frac{1}{\tilde{A}_1}\dot{u}_i^A\right)^{11}$$

$$\frac{\partial}{\partial\xi^2}\left(\frac{1}{\tilde{A}_2}\dot{u}_i^A\right) = \left(\frac{1}{\tilde{A}_2}\dot{u}_i^A\right)^{01} + \xi^1\left(\frac{1}{\tilde{A}_2}\dot{u}_i^A\right)^{11} \tag{B6}$$

This methodology plays a central role in derivation of the stiffness matrix with the help of the 3D analytical integration because allows us to calculate mode strain vectors $\boldsymbol{\varepsilon}^{s_1s_2}$ through the node displacement values and has been proposed by Kulikov and Plotnikova (2005, 2006, 2007).

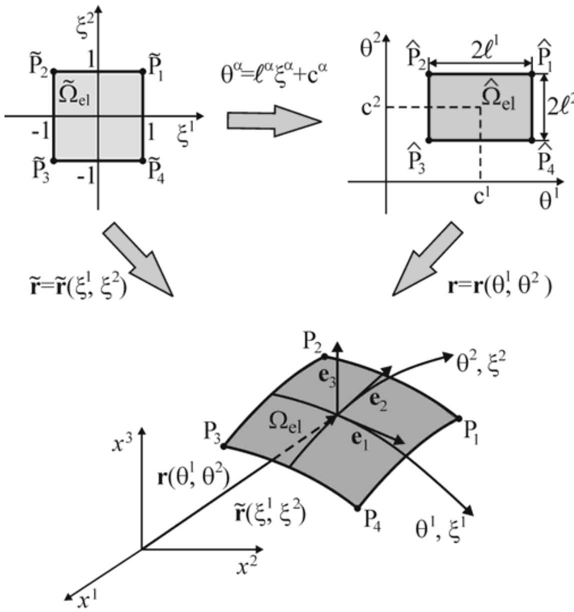


Figure B1: Biunit square in $\left(\xi^1, \xi^2\right)$ -space mapped into the geometrically exact four-node shell element in $\left(x^1, x^2, x^3\right)$-space

## Appendix C Some Remarks Concerning 3D Arrays

The *right* multiplication of a vector $\mathbf{U}$ of order 28 by a 3D array $\mathbf{A}^{s_1s_2}$ of order $10 \times 28 \times 28$ generates the matrix $\mathbf{A}^{s_1s_2}\mathbf{U}$ of order $10 \times 28$ whose elements are described by Eq. 56, that is,

$$\left(\mathbf{A}^{s_1s_2}\mathbf{U}\right)_{lp} = \sum_q A^{s_1s_2}_{lpq} U_q = \sum_q A^{s_1s_2}_{lqp} U_q \tag{C1}$$

since a symmetry condition (56b) holds. As we remember, the index $l$ runs from 1 to 10, whereas the indices $p$, $q$ run from 1 to 28.

We can also define the *left* multiplication of any vector $\mathbf{H}$ of order 10 by a 3D array $\mathbf{A}^{s_1s_2}$ of order $10 \times 28 \times 28$ following the rule:

$$\left(\mathbf{H}\mathbf{A}^{s_1s_2}\right)_{pq} = \sum_l A^{s_1s_2}_{lpq} H_l = \sum_l A^{s_1s_2}_{lqp} H_l = \left(\mathbf{H}\mathbf{A}^{s_1s_2}\right)_{qp} \tag{C2}$$

This implies that $\mathbf{H}\mathbf{A}^{s_1s_2}$ is the *symmetric* matrix of order $28 \times 28$.

There is a noteworthy transformation connecting right and left vector multiplications

$$\left(\mathbf{A}^{s_1s_2}\mathbf{U}\right)^{\mathrm{T}}\mathbf{H} = \left(\mathbf{H}\mathbf{A}^{s_1s_2}\right)\mathbf{U} \tag{C3}$$

The proof of this statement is trivial. Really, comparing the components of vectors in left and right parts of Eq. C3

$$\left[\left(\mathbf{A}^{s_1s_2}\mathbf{U}\right)^{\mathrm{T}}\mathbf{H}\right]_p = \sum_l \left(\mathbf{A}^{s_1s_2}\mathbf{U}\right)^{\mathrm{T}}_{pl} H_l = \sum_l \left(\sum_q A^{s_1s_2}_{lpq} U_q\right) H_l$$

$$\left[\left(\mathbf{H}\mathbf{A}^{s_1s_2}\right)\mathbf{U}\right]_p = \sum_q \left(\mathbf{H}\mathbf{A}^{s_1s_2}\right)_{pq} U_q = \sum_q \left(\sum_l A^{s_1s_2}_{lpq} H_l\right) U_q$$

one can see that both vectors are the same.

Finally, considering a matrix $\mathbf{K}_{\mathrm{H}}$ from Eq. 71 together with notations (57c) and a definition of the left multiplication of vectors of order 10 by 3D arrays $\mathbf{R}^{r_1r_2}$ from Eq. 62, we conclude that this matrix is symmetric.

## References

**ABAQUS** (1998): *ABAQUS Theory and User's Manuals*, Version 5.8. Hibbitt, Karlsson & Sorensen Inc., Rawtucket, Rhode Island.

**Atluri, S. N.** (1973): On the hybrid stress finite element model for incremental analysis of large deflection problems. *International Journal of Solids and Structures*, vol. 9, pp. 1177-1191.

**Atluri, S. N.; Liu, H. T.; Han, Z. D.** (2006a): Meshless local Petrov-Galerkin (MLPG) mixed collocation method for elasticity problems. *CMES: Computer Modeling in Engineering & Sciences*, vol. 14, pp. 141-152.

**Atluri, S. N.; Liu, H. T.; Han, Z. D.** (2006b): Meshless local Petrov-Galerkin (MLPG) mixed finite difference method for solid mechanics. *CMES: Computer Modeling in Engineering & Sciences*, vol. 15, pp. 1-16.

**Basar, Y.; Ding, Y.; Schultz, R.** (1993): Refined shear-deformation models for composite laminates with finite rotations. *International Journal of Solids and Structures*, vol. 30, pp. 2611-2638.

**Basar, Y.; Itskov, M.; Eckstein, A.** (2000): Composite laminates: nonlinear interlaminar stress analysis by multi-layer shell elements. *Computer Methods in Applied Mechanics and Engineering*, vol. 185, pp. 367-397.

**Basar, Y.; Kintzel, O.** (2003): Finite rotations and large strains in finite element shell analysis. *CMES: Computer Modeling in Engineering & Sciences*, vol. 4, pp. 217-230.

**Bathe, K. J.; Dvorkin, E. N.** (1986): A formulation of general shell elements - the use of mixed interpolation of tensorial components. *International Journal for Numerical Methods in Engineering*, vol. 22, pp. 697-722.

**Betsch, P.; Stein, E.** (1995): An assumed strain approach avoiding artificial thickness straining for a nonlinear 4-node shell element. *Communications in Numerical Methods in Engineering*, vol. 11, pp. 899-909.

**Bischoff, M.; Wall, W. A.; Bletzinger, K. U.; Ramm, E.** (2004): Models and finite elements for thin-walled structures. In: E. Stein, R. de Borst, T. J. R. Hughes (eds) *Encyclopedia of Computational Mechanics*. Vol. 2: Solids and Structures. Willey, pp. 59-137.

**Boland, P. L.; Pian, T. H. H.** (1977): Large deflection analysis of thin elastic structures by the assumed stress hybrid finite element method. *Computers and Structures*, vol. 7, pp. 1-12.

**Brank, B.** (2005): Nonlinear shell models with seven kinematic parameters. *Computer Methods in Applied Mechanics and Engineering*, vol. 194, pp. 2336-2362.

**Braun, M.; Bischoff, M.; Ramm, E.** (1994): Nonlinear shell formulations for complete three-dimensional constitutive laws including composites and laminates. *Computational Mechanics*, vol. 15, pp. 1-18.

**Cho, C.; Lee, S. W.** (1996): On the assumed strain formulation for geometrically non-linear analysis. *Finite Elements in Analysis and Design*, vol. 24, pp. 31-47.

**El-Abbasi, N.; Meguid, S. A.** (2000): A new shell element accounting for through-thickness deformation. *Computer Methods in Applied Mechanics and Engineering*, vol. 189, pp. 841-862.

**Hughes, T. J. R.; Tezduyar, T. E.** (1981): Finite elements based upon Mindlin plate theory with particular reference to the four-node bilinear isoparametric element. *Journal of Applied Mechanics*, vol. 48, pp. 587-596.

**Kim, Y. H.; Lee, S. W.** (1988): A solid element formulation for large deflection analysis of composite shell structures. *Computers & Structures*, vol. 30, pp. 269-274.

**Kulikov, G. M.** (2004): Strain-displacement relationships that exactly represent large rigid-body displacements of a shell. *Mechanics of Solids*, vol. 39, pp. 105-113.

**Kulikov, G. M.** (2007): On the first-order seven-parameter plate theory. *Trans. TSTU*, vol. 13, pp. 518-528.

**Kulikov, G. M.; Plotnikova S. V.** (2002): Simple and effective elements based upon Timoshenko-Mindlin shell theory. *Computer Methods in Applied Mechanics and Engineering*, vol. 191, pp. 1173-1187.

**Kulikov, G. M.; Plotnikova, S. V.** (2003): Non-linear strain-displacement equations exactly representing large rigid-body motions. Part I. Timoshenko-Mindlin shell theory. *Computer Methods in Applied Mechanics and Engineering*, vol. 192, pp. 851-875.

**Kulikov, G. M.; Plotnikova, S. V.** (2005): Equivalent single-layer and layer-wise shell theories and rigid-body motions. Part II. Computational aspects. *Mechanics of Advanced Materials and Structures*, vol. 12, pp. 331-340.

**Kulikov, G. M.; Plotnikova S. V.** (2006): Non-linear strain-displacement equations exactly representing large rigid-body motions. Part II. Enhanced finite element technique. *Computer Methods in Applied Mechanics and Engineering*, vol. 195, pp. 2209-2230.

**Kulikov, G. M.; Plotnikova S. V.** (2007): Non-linear geometrically exact assumed stress-strain four-node solid-shell element with high coarse-mesh accuracy. *Finite Elements in Analysis and Design*, vol. 43, pp. 425-443.

**Lee, K.; Cho, C.; Lee, S. W.** (2002): A geometrically nonlinear nine-node solid shell element formulation with reduced sensitivity to mesh distortion. *CMES: Computer Modeling in Engineering*

*& Sciences*, vol. 3, pp. 339-349.

**Pagano, N. J.** (1970): Exact solutions for rectangular bidirectional composites and sandwich plates. *Journal of Composite Materials*, vol. 4, pp. 20-34.

**Parisch, H.** (1995): A continuum-based shell theory for non-linear applications. *International Journal for Numerical Methods in Engineering*, vol. 38, pp.1855-1883.

**Park, H. C.; Cho, C.; Lee, S. W.** (1995): An efficient assumed strain element model with six dof per node for geometrically nonlinear shells. *International Journal for Numerical Methods in Engineering*, vol. 38, pp. 4101-4122.

**Sansour, C.** (1995): A theory and finite element formulation of shells at finite deformations involving thickness change: circumventing the use of a rotation tensor. *Archive of Applied Mechanics*, vol. 65, pp. 194-216.

**Schoop, H.** (1986): Oberflächenorientierte Schalentheorien endlicher Verschiebungen. *Ingenieur-Archiv*, vol. 56, pp. 427-437.

**Simo, J. C.; Rifai, M. S.; Fox, D. D.** (1990): On a stress resultant geometrically exact shell model. Part IV. Variable thickness shells with through-the-thickness stretching. *Computer Methods in Applied Mechanics and Engineering*, vol. 81, pp. 91-126.

**Suetake, Y.; Iura, M.; Atluri S. N.** (2003): Variational formulation and symmetric tangent operator for shells with finite rotation field. *CMES: Computer Modeling in Engineering & Sciences*, vol. 4, pp. 329-336.

**Sze, K. Y.** (2002): Three-dimensional continuum finite element models for plate/shell analysis. *Progress in Structural Engineering and Materials*, vol. 4, pp. 400-407.

**Sze, K. Y.; Chan, W. K.; Pian, T. H. H.** (2002): An eight-node hybrid-stress solid-shell element for geometric non-linear analysis of elastic shells. *International Journal for Numerical Methods in Engineering*, vol. 55, pp. 853-878.

**Sze, K. Y.; Liu, X. H.; Lo, S. H.** (2004): Popular benchmark problems for geometric nonlinear analysis of shells. *Finite Elements in Analysis and Design*, vol. 40, pp. 1551-1569.

**Timoshenko, S. P.; Goodier, J. N.** (1970): *Theory of Elasticity*, 3rd edition, McGraw-Hill, New-York.